CDP-ES-80-1
Issued 3/21/80
Copy No. 16

T. C. MERCER, JR.
C&P DEPT.
INFORMATION SERVICES
JACKSON LABORATORY

Distribution on last page.

EXPERIMENTAL STATION
RESEARCH AND DEVELOPMENT DIVISION TECHNICAL REPORT
CHEMICALS, DYES AND PIGMENTS DEPARTMENT
E. I. DU PONT DE NEMOURS & COMPANY

SURFACE CHEMISTRY OF TiO_2 - PART III

Work Done By:	Lloyd Abrams
Report Written By:	Lloyd Abrams
Approved By:	K. K. Bhatia
Patent Situation Approved By:	J. W. Heberling, Jr. Date 1/7/80
Previous Related Reports:	PTD-SA-78-1B, CDP-EX-78-15
Project Code:	7053-184084, 7053-184082
Type Technical Work:	IEB
Period Covered:	June 1978 - October 31, 1979
Notebook Nos.:	E13871, E16068, E16080, E16105, E16106
Personnel:	L. Abrams, R. E. Johnson, L. J. Janvier, J. V. Hughes, E. Z. Krams, P. R. Spring

ABSTRACT

We continued our research on the direct preparation of slurry from reactor discharge material; improved our understanding of the effects of surface alumina on colloidal properties and defined the restructuring of co-oxidized alumina on contact with water.

Significant differences in pigment surface chemistry were determined by adsorption/desorption of aluminum onto pigments in aqueous suspension. R-900 CD (base) adsorbs aluminum from >20 ppm solutions,

but R-960 does not adsorb any. This work indicates that modification of the alumina deposition on R-960 is a possible route to a high gloss, durable pigment permitting grade reduction/consolidation.

In related work, we found that R-960 has the same aggregate size as R-900 after micronizing, but it gradually agglomerates in suspension because of limited surfactant adsorption and surface coating solubility.

Research has continued to better understand the interactions between a pigment's surface and end-use systems. We have related pigment flocculation to surface chemistry, equilibrium pH, zeta potential and surfactant adsorption. As little as 1/4 of a monolayer of a strong anionic surfactant has a large influence on colloid stability. Adsorption of Tamol 731, which behaves like a simple anion, decreases with increasing pH and depends on pigment surface chemistry.

I. INTRODUCTION

The primary use of TiO_2 is to provide opacification which is related to its index of refraction and controlled particle size. Because TiO_2 pigments are composed of small particles with high surface area, surface chemistry governs their end-use performance.

For example, our durable pigment grades are coated with silica to effectively eliminate photo-reactivity problems. Some pigments are coated with alumina to make them more dispersible in many end-use systems. Some customer formulations require high volume loadings of our pigments. For these crowded systems, we coat our pigments with combinations of oxides to prevent the pigment particles from getting too close together. Such crowding would result in a loss of light-scattering efficiency. We alter the surface chemistry of some pigments during their manufacture to improve their processability. For example, small amounts of alumina are used to control agglomeration of slurries and improve their filtration rates. Knowledge of pigment surface chemistry is therefore important to TiO_2 production and its end-uses. Previous work in this area is reported in PTD-SA-78-1B and CDP-EX-78-15.

My program is to learn how to control the surface chemistry of our Ti-Pure® pigments and maximize their end-use performance. The motivation for this program is:

- to provide guidance and methods of product control to our process and product groups
- to resolve customer problems more efficiently
- to meet anticipated customer needs of future end-use chemical systems
- to provide our customers with counter-offerings that out-perform our competition
- to support our cost reduction program by reducing the number of grades, make the remaining grades compatible with more end-uses, and reduce mill-costs by making slurry directly from cyclone discharge.

II. OBJECTIVE

The objective of this study is to gain further insight into the surface chemistry of TiO_2 pigments and apply it to support the cost reduction and product improvement programs of White Pigments and Minerals R&D.

III. SUMMARY AND CONCLUSIONS

- Developed a working hypothesis describing the effects of surface alumina on pigment colloidal properties and then developed an improved understanding of co-oxidized alumina associated with TiO_2 and how it restructures upon contact with water. Measured the desorption/adsorbtion of aluminum by pigments in aqueous suspension. Found that R-900 CD (base) adsorbs soluble aluminum in concentrations >20 ppm whereas R-960 showed no sorption.

This work indicates that we should be able to make slurry directly using reactor discharge material.

- Developed rationale to relate pigment flocculation behavior to information about surface chmistry, equilibrium pH, zeta potential-pH character and surfactant adsorption. As little as 1/4 of a monolayer of a strong anionic adsorbent was observed to have a large effect on colloid stability. Measured adsorption of Tamol 731, a widely used anionic surfactant, and found adsorption decreased with increasing pH. Found that this drop-off trend relates to the pigment surface chemistry. Adsorption mechanism for Tamol appears similar to mechanism for simple anion adsorption.

This work provides the basis for understanding how a pigment surface interacts with end-use chemical systems.

- Found that R-960 (durable silica/alumina coated pigment) has the same aggregate size as R-900 (alumina coated) after micronizing. Determined that R-960 agglomerates in suspension with time because of the slow rate of surfactant adsorption.

This work indicates that the deposition conditions for alumina should be modified. If accomplished, a high-gloss, durable pigment can be made and grades consolidated.

- Began program to accelerate settling of Florida humate and eliminate need for extensive settling ponds.

- Found an alternate route to 'wet' R-101 using F- as flocculating agent instead of alumina.

- Began study of competitive pigments to identify micro-physical and chemical surface properties that determine end-use performance. This information would direct studies to making pigments with surfaces permitting broad acceptance in end-use classes, thereby permitting grade consolidation without loss of sales.

- A study of the surface modification of SDG was begun to improve gloss and viscosity stability of R-950 slurry.

IV. PATENT SITUATION

None yet.

V. PROGRAM

J. H. Boughton will continue portions of this study.

VI. PUBLICATION STATUS

None.

VII. SPECIAL SAFETY PRECAUTIONS

None.

VIII. ENVIRONMENTAL CONSIDERATIONS

None

IX. ACKNOWLEDGEMENT

The author gratefully acknowledges the close collaboration with R. E. 'Ted' Johnson (CR&DD) in doing most of this research. Discussions with John Boughton, Luis Matienzo and Dave Schussler were quite helpful. The excellent lab work of Dolly Janvier, Jerry Hughes, Ed Krams and Paul Spring in doing the described experiments were indispensable to the author.

TABLE OF CONTENTS

X. EXPERIMENTAL AND DISCUSSION

A. Restructuring of Surface Alumina

While using zeta potential as one of the techniques to characterize R-900 cyclone discharge, R. E. Johnson and I observed that the zeta potentials shifted with time. This phenomenon is illustrated in Figure 1. The "initial" curve is the zeta potential-ph curve for the R-900 CD (cyclone discharge) "as received". After some time (hours) in aqueous suspension (at the pH's indicated, room temp., and in plastic containers) the zeta potential values climbed to give the curve "after exposure".

By combining this observation with the information from the open literature (for example, Healy, Parfitt, etc.) and the work of Prof. L. L. Hench (consultant), J. H. Boughton and others, we developed a definitive picture of the chemistry involved for understanding the effect of Al (from co-oxidation) on the behavior of aqueous slurried R-900 CD.

In essence, we observed that aluminum dissolves from pigment surfaces. Depending upon the suspension (slurry) conditions (pH, temperature, ions and other chemical species present, time of contact, etc.), we discovered that the aluminum in solution will polymerize to some degree and the polymeric alumina adsorbs back onto the particles. This process (surface aluminum dissolution, polymerization and adsorption of polymer) allows the alumina-containing-surface to restructure and accounts for most of the previously reported differences in measurements shown in Table I.

TABLE I

EFFECTS OF SURFACE ALUMINA RESTRUCTURING

- Heterogeneous Distribution of Al from Coox (JHBo, R.Davies)
- Change of Zeta Potential with Time (REJ)
- Heating Effects on Zeta Potential (LLH & AA)
- Bi-Modal Zeta Potential (LLH)
- Precipitation Order for Coatings (AA)

...Heterogeneous Al distribution. John Boughton has observed that a significant fraction of pigment base (1% co-oxidized Al_2O_3) particles have little or no surface aluminum. When Al-free TiO_2 particles are put into an aqueous suspension containing a few ppm of Al ions, they readily adsorb aluminum species (Parfitt, TWHealy). Soluble Al species coming from Al-rich TiO_2 particles are present in ample supply (as shown by our previous work) to adsorb and raise the IEP of Al-free TiO_2 (rutile) particles (5.4) to that reported for R-900 cyclone discharge (7.0).

If slurry conditions are such that more Al is available for adsorption, larger zeta potential shifts are observed. For example, Figure 2 shows the zeta potential histrogram of R-900 cyclone discharge particles in pH 5 water. The distribution in zeta potentials is, at the least, bi-modal. By far, the largest number of particles are centered around a potential of +20 mv with a distinct 2nd distribution at 35-40 mv. The histogram was obtained within 4 minutes after making the aqueous suspension. If the same particles were suspended in the supernatent of a more concentrated slurry or if sufficient Al^{+3} were added, the bi-modal (or tri-etc.) histogram shown in Figure 2 would disappear with the lower zeta potential peaks shifting upwards to the 35-40 mv range.

The shifts in zeta potentials were monitored over the entire pH range and the new zeta potential histogram values vs. pH approached those obtained for R-900 (3% alumina coated product) as shown in Figure 1. At higher pH's, bi-modal zeta-potential distributions were not observed. The dissolution/adsorption process at pH >7 may be too fast for the present zeta meter (Pen Kem, System 3000) to follow.

Figure 4 shows a comparison of Zeta Potential measurements for R-900 CD with those for a chemically cleaned R-900 CD as described in a previous report (1). Curves Cϕ/24A·REJ and Cϕ24A·LLH are the zeta potential-pH measurements reported by R. E. Johnson and L. L. Hench for the same R-900 CD (Cϕ24A) sample. Curve ·REJ represents samples obtained by dispersing the R-900 CD in water at the desired pH and diluting the suspension in water at that pH. Curve ·LLH represents R-900 CD dispersions that were first centrifuged and then a small portion of the sediment was redispersed in the supernatent. By invoking the Al solution/adsorption mechanism, the difference in zeta potential-pH curves is readily explained. The data points (*) for the chemically cleaned R-900 CD are for particles remaining in the supernatent of a concentrated slurry at that pH. The Al in solution is sufficient to adsorb onto the particles and reproduce the ·LLH curve. The zeta potential-pH curve for the sediment duplicated the ·REJ curve because of an insufficient Al supply.

...Change of Zeta potential with time. R. E. Johnson has observed changes occurring on the order of weeks and months. Such changes are measurable in terms of modifications in structure of polymeric alumina gels on the particle surface.

...Heating effects on Zeta potential. These affects were observed by L. L. Hench and A. Allen. Pronounced changes in alumina chemistry (gel → transition oxide → stable oxide) are known to occur upon heating. Shifting in ZP-pH curves, therefore, seems reasonable; furthermore, the alumina-gel structures readily take up transition metals which the R-900 CD has (2) and the slow zeta potential shift with time may reflect the slow incorporation of these metals.

...Bi-Modal Zeta Potential. Prof. L. L. Hench has reported bi-modal zeta potential distributions. As shown in Figures 2 & 3, a bi-or maybe tri-) modal distribution was observed at pH 5. These distributions were not observed for higher pH preparations, possibly because the measuring speed of the zeta meter is too slow. A bi-modal system might be observed for a non-aqueous system or with shorter measuring times of the zeta potential for the pH range >7.

...Precipitation order for coatings.
making quality pigments by first depositing an alumina coating followed by a silicate coating. The 'first' alumina coating may homogenize the surface presented and make subsequent coating operations more uniform.

B. Zeta Potential Histograms

Reliable histograms of the number of particles (several thousand) at a zp vs pH are now available using the Pen-Kem system 3000 and Figure 5 shows the effect of pH on the histogram shape and position for the 'clean' R-900 CD. The width of the histogram may provide information concerning the uniformity of the surface. The width was ∿ 5-7 mv for R-900 CD in the pH 6-7.5 range and increased to 15-25 mv outside that range.

For R-900 (3% hydrated alumina content), the histogram widths were much narrower (less than 1/2 of the R-900 CD values) and may reflect its more homogeneous surface. Additional work needs to be done to get some use out of these histograms.

C. Analysis of Soluble Aluminum

A modification of a CD&P analytical method, No. W200.015, was used to measure soluble aluminum, and a copy of the modification is included in the Appendix. Essentially, the aluminum in

solution is converted to a colored-complex and the UV absorbance (optical density) is obtained as a function of Al concentration. A linear calibration was obtained for the concentration range 0-7 ppm aluminum and is shown in Figure 6.

R-900 and "clean' R-900 CD suspensions were prepared in pH 4 water. The aluminum contents were measured 1 and 24 hours after suspension preparation and the results are summarized in Table II.

Table II

Al-Contents in Aqueous Suspensions of TiO_2

pH - 4

Pigment	Time Hours	ppm - Soluble Al Suspension Concentration - % TiO_2 1	0.1	0.01
R-900	1	1.292	0.505	0.188
R-900	24	1.019	0.492	0.236
R-900 CD	1	1.220	0.338	0.133
R-900 CD	24	1.369	0.467	0.176

These measurements show that considerable Al dissolves from these pigment surfaces and supports the hypothesis for the observed changes in surface alumina chemistry. Furthermore, the dissolution process is rapid (over in less than 1 hr) and similar for both materials (almost equivalent surface areas). This measurement shows that water provides the transfer medium for the alumina surface (from cooxidation) to restructure. By better definition of suspension conditions, a slurry product might be made directly from cyclone discharge material.

Aluminum adsorption experiments were run using R-960 (C104E) and "as received" R-900 CD (C104C). The results are shown in Table III.

0-80 ppm of aluminum was added to a suspension containing 1% pigment. At 0 ppm added aluminum, both pigments show considerable Al desorption: ∿8 ppm from R-900 CD and 5+ ppm from R-960.

For R-900 CD, the measured amount of soluble aluminum tracks the amount added + 8 ppm for the samples where 1 to 10 ppm Al was added. For the samples where the amount of added aluminum was >20 ppm, adsorption of aluminum became significant at 80 ppm.

Table III

Al Sorption (ppm) on R-900 CD and R-960 at pH 3

Room Temperature

Al Added(1)	R-900 CD (C104C) Total(2)	R-900 CD (C104C) Diff.(3)	R-900 CD (C104C) Amt. Sorbed(4)	R-960 (C104E) Total(2)	R-960 (C104E) Diff.(3)
0	7.9	7.9	0	6.0	6.0
1	9.7	8.7	0	6.1	5.1
2	9.9	7.9	0	7.1	5.1
4	11.7	7.7	0	8.5	4.5
10	18.5	8.5	0	14.5	4.5
20	26.7	6.7	1.2	25.2	5.2
40	46.6	6.6	1.3	44.9	4.9
80	81.6	1.6	6.3	86.1	6.1

Note: (1) Al conc., ppm, added to suspension
(2) Measured Al conc. in supernatant
(3) = (2) - (1)
(4) Al, ppm, adsorbed onto surface: For R-900 CD, (4) = 7.9 - (3)

The measurements for R-960 show no aluminum adsorption for the 1-80 ppm range. The Al-desorption/adsorption behavior of R-900 CD and R-960 confirms that the surfaces are quite different chemically. The sorption of Al by R-900 CD lends support to our concept of transforming its surface in slurry form. On the other hand, the lack of sorption by R-960 shows that the presence of silica greatly influences its surface reactivity.

The aluminum adsorption experiments should be continued at higher pH's, temperatures and loadings to determine if the surfaces of R-900 CD and R-960 can be restructured to one similar to that of R-900. The specific effects of anions, e.g. $CO_3^{=}$, $SO_4^{=}$, Cl, etc.,

should also be examined with respect to controlling surface coating chemistry (3). Another set of experiments should involve restructuring of high 2-3% Al co-ox containing material including a step for surface hydrolysis (H_2O exposure at elevated temperatures) before slurrying.

D. R-950 Slurry

R-950 slurry is made from SDG (simultaneous drying and grinding) base and exhibits gloss and viscosity instability upon aging. This instability may be caused, in part, by the lack of a stable surface coating on the SDG base such as the 3% hydrated alumina coating deposited on R-900. To check this hypothesis, TiO_2 pigment was recovered from R-950, washed, and zeta potential-pH measurements were made.

Shown in Figure 7 are the zeta potential-pH curves for:

- the recovered pigment in Tamol suspension (solid line)
- the same pigment but washed with deionized water to 140,000 ohms (Δ)
- the same pigment, washed 6 times with 0.1 N NaOH and then with H_2O to >5000 ohms (+)
- R-950 base (SDG pigment)

The IEP curve (zeta potential vs pH) for the pigment/Tamol suspension shows that R-950 base (SDG) readily adsorbs this surfactant. After water leaching, the Tamol SG-1 is still present on the surface and the IEP curve is shifted half-way between the curves for the pigment/Tamol and SDG suspensions. Drastic leaching, 0.1N NaOH, removes more of the Tamol as shown by the shift in IEP but does not remove it completely.

It is possible that the strongly adsorbed Tamol SG-1 surfactant may not be easily displaced by the surfactant-of-choice in some end-use systems. The presence of other surfactants may cause the dispersed pigment particles to associate (floc or bridge) because of interactions of the residual strongly adsorbed surfactant.

SDG material was treated with caustic to improve the stability of the resulting R-950 slurries. The results are shown in Table IV.

TABLE IV

R-950 PERFORMANCE - DESOTO 7811

AGING AT 140°F

			60° Gloss			Brookfield #5 Spindle					
						Initial		2 Wks		3 Wks	
		Treatment	Initial	2 Wks	3 Wks	10 RPM	100 RPM	10 RPM	100 RPM	10 RPM	100 RPM
R-940	4507	Control	38	39	36	7,600	1,680	9,600	2,200	10,400	2,480
R-950	TR-93584	Control	42	34	32	4,800	1,120	7,600	1,760	8,400	2,040
R-950	E16106-54C	NaOH, Room Temp.	36	31	30	5,200	1,260	7,600	1,960	8,800	2,280
R-950	" -54D	NaOH, 60°C	38	34	33	3,800	980	5,800	1,560	6,800	1,820
R-950	" -56C	NH_4OH, Room Temp.	41	37	36	3,600	900	5,400	1,520	6,200	1,680
R-950	" -56D	NH_4OH, 60°C	40	35	35	3,800	1,020	5,800	1,600	7,200	1,940

Treatment of SDG material by either caustic at pH 8.5 produces R-950 slurry with lower viscosity and reduced-loss-of-gloss upon aging at 140°F. NH_4OH treatment seems to give a higher gloss and lower viscosity than the corresponding NaOH-treated SDG. Heating the SDG at 60°C, pH=8.5, showed no improvement in slurry stability.

Two other experiments should be run:

- R-900 used instead of SDG to make up R-950. If the gloss instability approaches that obtained with SDG, then the surfactant package is probably responsible.

- Glass containers are currently used in the aging test. We have found considerable silica migration at room temperature (in one day) from glass to pigment surfaces in our zeta potential studies. To eliminate this possible testing artifact, plastic containers should be used.

One additional point should be noted: the viscosity of all the slurries, including R-940 made from R-900, increased markedly during the three week aging test. If replacement of the glass containers by plastic does not eliminate this increase, then it may be caused by either alumina or the surfactant system. If it is alumina, then ways will have to be found to stabilize the surface. On the other hand, the surfactant system could either degrade or bridge particles; both mechanisms would increase viscosity.

The experiments performed, therefore, seem to show that control of the alumina surface has a desirable effect by reducing initial viscosities. However, the % increase in viscosity on aging at 140°F was the same for the caustic treated and non-treated SDG samples. The viscosity of R-940 increases similarly upon aging and therefore strongly indicates that aluminum gels of same sort may be forming in the liquid. This problem should be studied in conjunction with restructuring the alumina surface.

E. Particle Size Measurements of Pigment Dispersions

The transient turbidity apparatus of Dr. C. M. Paulson (Engg) was successfully evaluated and setup in R. E. Johnson's laboratory (4). Transient turbidity is a size measuring technique complementary to the sedigraph. Listed in Table V is a comparison of the two techniques.

Table V

COMPARISON OF SEDIGRAPH VS TRANSIENT TURBIDITY

System	Time/Run	Suspension Stability	TiO_2 Level	Limits
Sedigraph	30-90 min.	Stable	2%	particle size must be >0.3 μm
Transient Turbidity	10 sec. 1 min + prep. time	Stable and unstable	0.005%	solution conductivity must be <100 μm

The sedigraph is extremely useful in obtaining particle size distributions of pigments. Its main drawbacks are the long times (30-90 min) required per analysis and that distributions for particles below 0.3 μm will be in error because of Brownian motion. It can readily handle slurries with 1-2% pigment concentration in the presence of surfactants, etc.

The transient turbidity apparatus uses light transmission as a monitor and therefore requires very dilute TiO_2 pigment suspensions. Furthermore, because it uses an electrical voltage to align the particles' rotation, the conductivity of the pigment dispersion is limited to 100μ mho to prevent thermal currents, etc. The electrical measurement takes a few seconds and its conversion has been calibrated for a log-normal distribution in diameter (weight) and its standard deviation.

Shown in Figures 8 and 9 are particle size measurements for R-900 and R-960 aqueous Tamol 731 suspensions @ pH 10, using the transient turbidity and sedigraph techniques, respectively. By measuring particle size as a function of time, we observed that R-960 agglomerates from 0.42 μm at 2 minutes to 0.50 μm at 30 minutes, even though the zeta potential of the particles is highly negative. After ~ 30 minutes, the agglomerate size of R-960 is reasonably stable. Corresponding sedigraph measurements give sizes of 0.51 for R-960 and 0.41 for the R-900.

The agglomerate size changes for R-900 and R-960 could not be monitored by the sedigraph which requires at least 30 minutes for a measurement. The size instability and agglomerate growth of R-960 in an aqueous Tamol suspension may be responsible for its low gloss in some paint formulations. Furthermore, the transient turbidity size measurement for R-960 extrapolates to the same size as R-960,

~0.38 μm, at zero suspension time or when these pigments came out of the micronizer. Thus the micronizer is able to grind R-960 down to the same aggregate size as R-900 but the R-960 surface is probably not as well-stabilized as R-900's.

Figure 10 shows the transient turbidity size measurements for:

Commercial R-900

Laboratory prepared 'boehmite'-coated-R-900'

Laboratory prepared 'bayerite-coated-R-900'

in Aqueous/Tamol 731 suspensions. The commercial grade of R-900 and the lab prep are similar as expected. The bayerite-coated pigment keeps on agglomerating under the same conditions in which the boehmite surface is stable. Thus, transient turbidity size measurements might provide a rapid method of predicting a pigment's gloss and stability in end-use systems.

Shown in Table VI are transient turbidity size measurements for various pigment grades.

Table VI

TRANSIENT TURBIDITY SIZE MEASUREMENTS OF AQUEOUS PIGMENT SUSPENSIONS

NO SURFACTANTS[1]

Material	pH	Size, μm[2]	
R-900 CD[3]	6.3	0.97	
R-900 CD (SM)[4]	4.6	0.40	
R-900 DD[5]	6.2	0.62	
R-900	10.4	0.415	3% Al
RPS CD	6.3	0.90	
R-960 DD	6.8	1.03	
R-960	4.8	0.49	6% Si, 2% Al
			% Si % Al
R-902-08 (Lot 9256)	10.2	0.46	1 1/2 3
R-931-01 (Lot 6639)	8.2	0.62	8 7
R-933-01 (Lot 7230)	10.3	0.67	10 7
R-994 (Lot 9749)	9.5	0.54	
LW (Lot 5250)	4.1	0.63	

Notes: (1) HCl, NaOH used to adjust pH; suspensions were sonicated
(2) Stable, smallest agglomerate size
(3) CD; cyclone discharge, unground
(4) SM; steam micronized
(5) DD; dryer discharge

Within experimental error, the size of CD materials, R-900 CD and RPS CD (EM base), was measured at 0.9 μm. Under extended sonication and high pH conditions, the size of the CD materials was somewhat reduced to 0.6-0.7 μm. Steam micronization at 3:1 S/P ratio, of the R-900 CD reduced the agglomerate size down to 0.40 μm. The agglomerate sizes for R-900 DD and R-960 DD were 0.62 μm and 1.03 μm, respectively. This size difference may relate to the tendency of R-960 to agglomerate and therefore may provide a good measure of the effectiveness of the alumina hydrate coating.

The agglomerate sizes of R-900 (3% hydrated oxide), R-902 (4 1/2%), R-960 (8%), R-931 (15%) and R-933 (17%) are directly dependent on the amount of their hydrous oxide coatings as shown in Figure 11. One of the functions of these coatings seems to be to stabilize the 'primary aggregates' of 0.4 μm into larger sized agglomerates. The extrapolated value of 0.36 μm for uncoated particles is within the accepted size range for the 'primary aggregate'. From this size and the measured sizes of the various coated products, the number of primary aggregates per agglomerate may be calculated and Table VII summarizes the results.

Table VII

ESTIMATED NUMBER OF 'PRIMARY AGGREGATES'
PER STABLE AGGLOMERATE
CALCULATED FROM TRANSIENT TURBIDITY MEASUREMENTS

Material	Number of Primaries (±5%)
R-900	1.50
R-902	2.0
R-960	2.5
R-931	5.0
R-933	6.0

If these numbers are significant, then the coatings may well function as size adjusters (controlled clumping).

F. Competitive Pigments

There is a lack of physical and chemical information on competitive pigments (other than standard pigments data). At present, we cannot relate a pigment's end-use performance to its physical and chemical properties. Therefore we do not know what those properties should be to maximize a pigment's performance. Our efforts in product improvement would be better spent in defining the end-use performance of pigments in terms of their readily measurable physical and chemical properties.

If, for example, we could define and make a specific type of hydrated alumina surface for R-900 that would be acceptable by most of our customers, we could reduce costs by eliminating many of the package codes presently required. Another example of cost reduction might be definition of the target hydrated alumina surface required for the reactor discharge slurry product and its counterpart dry grade. Therefore, if we learn what pigment properties are important and how they control end-use performance, this information will then be used to guide our product improvement and cost reduction programs.

As a first step to providing these relationships, we have started to catalog those properties which appear to control performance in specific end-uses. To accomplish this we are compiling property-performance data of competitives as well as our pigments according to their chief end-uses. Table VIII is a partial list of pigments collected and some of their properties measured-to-date.

Table VIII

COMPETITIVE PIGMENT ANALYSIS

Grade	TC#	% SiO_2	%Al_2O_3	S.A., M^2/G	Size, µm
Titanox 2090	9089	nil	2.7	13.9	0.42
Titanox 2131	9090	9.5	4.9	41.7	0.58
Unitane OR580	9091	0.1	2.4	17.3	0.40
Tronox CR800	9092	0.1	1.9	11.1	0.38
Tronox CR820	9082	2.1	2.4	11.7	0.38
Tronox CR822	9088	3.3	3.1	14.1	0.45
Titanox 2020	9104	nil	3.1	13.9	0.38
Tioxide RHD6U	9086	0.1	2.9	18.6	0.35

The % SiO_2 and Al_2O_3 were measured by X-ray fluorescence using an Exam-6. The surface area measurements were done by CR&DD using BET N_2 adsorption-desorption data. The pigment particle sizes were calculated using transient turbidity measurements on stable aqueous pigment suspensions (sonicated).

Using the relationship shown in Figure 11, which was developed for Du Pont Ti-Pure® pigments, and the total % of hydrous oxides noted in Table VIII, the expected aggregate size (from Figure 11) is, within error, the size that was measured.

Zeta potential vs pH measurements (IEP curves) were performed on CR&DD's new system 3000 instrument and are shown plotted in Figures 12-18.

The iso-electric point (IEP) curves for some Du Pont pigments are shown in Figure 12. The transition in IEP of 4.5 to 9.0 for the grades shows the effect of an alumina coating (IEP 9) vs a silica coating with an IEP of 2.

Shown in Figure 13 are the IEP curves of some chalk-resistant paint grades. Except for the R-902 curve, the IEP curves are very similar and indicate that they probably have similar alumina-silica coatings. Furthermore, particle size measurements indicate that the competitives are all about 0.45 μm in size. Therefore, any differences in end-use performance such as gloss, dispersion and hiding power are probably caused by surface chemical factors. By using adsorption, ESCA and other measurements, we hope to isolate and define these factors for each end-use and establish standards for that end-use.

Shown in Figures 14 & 15 are the IEP curves of some enamel grades. The competitives have similar compositions, 0.1% SiO_2 and 2% Al_2O_3, and IEP curves. Most of the enamel grades have sizes in the 0.38-0.42 μm range with the notable exception of Tioxide's RHD6U which is 0.35 μm as measured by transient turbidity.

IEP curves for competitives are very similar for other end-uses as shown in Figures 16, 17 & 18. Again, specific performance differences are probably caused by surface chemical factors which have not, as yet, been defined.

Dispersion appears to be an end-use parameter with the widest range of values achieved using commercially 'good performing' pigments. Differences in dispersion quality are probably caused by pigment surface composition. By using adsorption, ESCA and other techniques, we hope to identify those factors which control performance in each end-use and optimize the surface composition to establish new performance standards and product recipes for each end-use.

G. Tamol Adsorption Studies

Surfactants are widely used in pigment end-uses to improve dispersibility, gloss and stability. In order to understand how these properties depend on surfactant/surface interaction, adsorption measurements of an anionic surfactant, Tamol 731, were obtained for a variety of materials under differing suspension conditions.

When pigment particles are dispersed into water, the instantaneous pH of their electrical double layers is probably close to the pigment's equilibrium pH value.* The zeta potential of a powder when first put into water is probably close to the value associated with the equilibrium pH. As the powder surface equilibrates in pH with its surroundings, its zeta potential changes. If the particles are forced to go through zero zeta potential, flocculation (agglomeration) may occur. Flocculation will occur if the adsorption of surfactant or other species is slow such that the rate of zeta potential change is also slower than the rate of flocculation. Furthermore, if the powder is heterogeneous, different rates of zeta potential modification by adsorption can occur; again leading to flocculation if both positive and negative or near zero zeta potential particles are present.

The discussion of the results for R-900 can serve as a general model. At its equilibrium pH of 7.4, R-900 particles have a zeta potential of 37 mv; designated as point E in Figure 19. When 1% R-900 is put into pH 4 water, the final suspension pH becomes 5.2 and the zeta potential of the particles moves from 37 mv @ point E to 54 mv @ point A. In this case, the zeta potential of the particles was always >+30 mv, signifying that they should be stable with respect to flocculation. Size measurement of R-900 by transient turbidity confirms this.

When R-900 is dispersed in pH 10.5 water (NaOH used to adjust pH), the zeta potential of the particles shifts from +37 mv @ point E to -35 mv @ point B. Flocculation should occur if this change in zeta potential is slow (on the order of 10-20 seconds). Transient turbidity shows that flocculation has occurred with about 2 aggregates per floc. Thus flocculation occurs rapidly (<1 sec) and the system is quite stable by the time the transient turbidity measurement is made. The change in floc size as measured by transient turbidity can provide an estimate of the order of magnitude of the rates of zeta potential modification and of the adsorption process.

Curve CD&P in Figure 19 represents the zeta potential-pH for an R-900 suspension containing Tamol 731. By considering only the final zeta potential values, which are highly negative, one would expect that the resulting suspensions would be very stable and not flocculate. If we assume, however, that the instantaneous pH of the

*Equilibrium pH is measured by titrating a powder into water. The pH at which no further change occurs upon addition of more powder is defined as the equilibrium pH (Prof. L. L. Hench).

R-900 powder particles when first put into suspension is near their equilibrium pH, 7.4 (point E, with an associated zeta potential of +37 mv), then flocculation might occur if:

* the rate of zeta potential change is slow when passing through or near zero

* the particles are heterogeneous, providing different adsorption rates and resulting in a suspension with both (+) and (-) charged particles.

When R-900 is put into an aqueous Tamol solution at pH 4, the zeta potential of the particles shifts from +37 mv at point E to -50 mv at point C (Figure 19). Transient turbidity shows that some flocculation, about 40%, occurred. The amount of flocculation for this case is ~1/2 as large as for the aqueous pH 10 suspension. The adsorption of Tamol on the alumina coating and attendant zeta potential change at pH 4 is faster than the OH^- sorption process at pH 10.

No measurable flocculation occurs when R-900 is dispersed in a pH 10/Tamol solution. The adsorption/zeta potential modification process is much more rapid than flocculation. The alumina coating, therefore, provides a homogeneous, uniform surface that rapidly adsorbs anions to allow particles to migrate quickly through large zeta potential changes together, thereby minimizing flocculation.

A similar rationale explains most of the data for R-960 shown in Figure 20. When R-960 is added to pH 4 water, the pH of the resulting 1% suspension is 7.5, point A, because of the high basic titer of the pigment. This pH is close to the IEP of R-960 and massive flocculation occurs. When placed in pH 10 water, the OH^- sorption/zeta potential modification is somewhat rapid and little flocculation occurs.

On the other hand, when R-960 is dispersed in aqueous/Tamol suspensions, flocculation is observed throughout the entire pH range studied. Tamol does adsorb on the R-960 as indicated by the shift of zeta potential-pH curves in Figure 20. However, flocculation is more extensive for R-960 than for R-900 for the same water/Tamol system. The difference in degree of flocculation suggests that the hydrated alumina surface of R-900 adsorbs Tamol more rapidly and uniformly than the silica-alumina surface of R-960. Furthermore, the addition of alumina in the R-960 coating process does not produce a surface with the reactivity of R-900. The combination of techniques (transient turbidity, zeta potential/pH, equilibium pH) can provide a qualitative definition of the desired surface chemistry and reactivity for a specific end-use surfactant system.

The adsorption of Tamol 731, an anionic surfactant, was measured for a variety of pigments and powders because it is widely used by our customers and is the basis of our aqueous emulsion gloss test. Instead of using ion chromatography as previously done (4) to follow Tamol adsorption, UV absorbance measurements were used. A plot of UV absorbance vs ppm Tamol in aqueous solution was developed, as shown in Figure 21, by monitoring the absorbance of a peak @ ~205 nm. Association of the Tamol at concentrations above 250 ppm is evident from this calibration curve. For this reason, only the linear portion of the curve in the 0-200 ppm range was used. More concentrated solutions were diluted to this range. The calibration curve is shown in Figure 22.

Shown in Figures 23-26 are the Tamol adsorption data, shown as langmuir isotherms, as functions of pH for R-900, R-960, R-900 CD and R-900 CD (steam micronized). All of these materials adsorb much more Tamol at pH 3 than they do at higher pH's. Figure 27 shows the R-900/Tamol adsorption-pH profile whose drop-off is typical for the materials. The adsorption drop-off is probably caused by the displacement of Tamol by OH^- at high pH or by a decrease in the number of adsorption sites.

The data were replotted as the amount adsorbed in a monolayer as a function of pH in Figure 28. The data were fitted with a least squares straight line. The drop-off in Tamol adsorption is similar for the alumina-only powders, R-900, R-900 CD and R-900 CD (steam micronized). R-960 behaves quite differently and has a much faster drop-off than the alumina-only powders. The presence of silica seems to interfere with anion adsorption processes.

The adsorption-pH curves for Tamol and simple anions (F^-, $SO_4^=$, Cl^-) on R-900 CD are shown in Figure 29. The slopes of the two curves are parallel and suggest that the same adsorption mechanism is operating. The R-960 data is shown for reference and its different fall-off is apparent.

The effect of Tamol adsorption on zeta potential was measured for R-900, R-900 CD, R-900 CD (sm) and R-960 for the pH range 3-11. Shown in Figure 30 is the data for R-960 at pH 3. This information is useful in predicting if flocculation should occur. As more Tamol is added, >40 ppm, the zeta potential drops below +30 mv and flocculation occur. In the region 40-250 ppm Tamol, the zeta potentials are in the flocculation range. Above 300 ppm Tamol adsorbed, the zeta potential is sufficiently negative to inhibit flocculation if adsorption rates are first.

Shown in Figure 31 are the corresponding size measurements for the samples used to make Figure 30. The adsorption-zeta potential-size rationale is, qualitatively, as predicted. This rationale operates throughtout the pH range studied and for the other materials.

Tamol adsorption was measured for Minusil silica, surface area ~3.5 m^2/g. Within experimental error, hardly any Tamol was adsorbed; almost 100 times less (per unit area) than R-960. It appears that R-960 does not behave like silica with respect to Tamol adsorption.

Future experiments should provide definition of the desired surface coating(s) for various grades by comparing Tamol or ion adsorption of competitives that disperse well in a wide range of end-uses.

H. Miscellaneous Studies

* Florida Humate settling. We showed that $FeCl_3$ added to a humate suspension at pH 5 raised the zeta potential from -21 mv to ~0 mv and caused flocculation. $FeCl_3$ might be added directly in the dredge pond, eliminating the need for settling and finishing ponds. Lab experiments are needed to show that floc rates and volumes are better and smaller than corresponding ones for H_2SO_4.

* Began ion adsorption study of $PO_4^{\equiv}$. Since we are co-oxidizing PCl_3 with $TiCl_4$ to make RPS, the resulting chemical state of phosphorous on the surface has had pronounced effects on viscosity. A program was just initiated to study phosphate adsorption to provide insights into JV-EM base differences, etc. Phosphate contents of RPS suspensions were obtained by ion chromatography for A. Baidins to aid his rheology studies.

* An analytical technique using ion chromatography was developed for E. W. Gillow and S. A. Hallock to measure the sulfate content of sales grade $FeCl_3$ (5). Mixed acid analysis (HNO_3/H_2SO_4) was also demonstrated for R. W. Craft (Repauno).

* With K. Kirksey, developed an alternative route to 'wet' R-100 & R-101 using F- as a flocculating agent instead of hydrous alumina.

XI. REFERENCES

1. Interim Report: L. Abrams, CDP-EX-78-15, "Surface Chemistry of TiO_2-II".

2. TiO_2 Product Development Report, L. Abrams, PTD-SA-78-18, "Chemical Characterization of TiO_2 Pigment - I".

3. G. Bardossy & J. L. White, Science 203, 355-6 (1979).

4. Memo to F. J. Darnell from R. E. Johnson & L. Abrams, May 8, 1978.

5. Notebook E17895-39, 1978

XII. APPENDIX

DETERMINATION OF Al Ions

PYROCATECHOL VIOLET COLORIMETRIC METHOD

I. APPLICABILITY

This method is applicable to sample solutions containing 0-10 ppm.

II. PRINCIPLE

The sample is dissolved by heating with HCl. Hydroxylamine hydrochloride and 1,10-phenanthroline are added to reduce and complex iron and prevent its interfering. Pyrocatechol violet is added to form a colored Al complex. After pH adjustment, absorbance at 585nm is measured to determine Al concentration.

III. UNUSUAL SAFETY CONSIDERATIONS

Handle glacial acetic acid with care. Conduct all work in a hood. Wear rubber gloves and an apron, avoiding all contact with the skin and inhalation of vapor. MAC in air is 10 ppm.

IV. SENSITIVITY, PRECISION AND ACCURACY

The smallest amount of Al detectable by the method is approximately 0.5 µg. Precision and accuracy have not been measured.

V. APPARATUS AND REAGENTS

(Equivalent apparatus may be substituted. Reagents are reagent grade.) Use deionized water throughout procedure.

1. Visible spectrophotometer capable of measuring absorbance at 585nm through a 10mm cellpath (20 or 50mm cells preferred for samples containing less than 0.1ppm Al).
2. pH meter
3. Acetic acid; dilute conc. acid 50% by weight
4. Aluminum standard solution, 1 ml = 1 mg. Al. Fisher Scientific Co., No. So-A-442 or make up 1000 ppm standard Al^{+3} at pH = 3.
5. Aluminum Working Standard: 10 ppm Al. To 1.000 g of 1000 ppm standard solution, add 1.00 g conc. HCl and dilute total to 100.0 g with distilled (deionized water). PREPARE FRESH FOR EACH CALIBRATION PROCEDURE.

6. Ammonium acetate solution; 10% (by weight) in H_2O.

7. Ammonium hydroxide solution; dilute conc. base 50% with H_2O.

8. Hydroxylamine hydrochloride solution, 20% (by weight) in H_2O.

9. 1,10 phenanthroline solution; 0.30 gm/100 g H_2O solution.

10. Pyrocatechol violet solution; " " " "
Also known as catechol violet, pyrocatechol sulfone phthalein.

VI. STANDARDIZATION

1. Take 7-250 ml beakers (preferably Teflon®) with stirring bars. Weigh out 1.000, 2.000, 4, 6, 8 and 10.000 g of 10 ppm Al working standard into six beakers (1 beaker is a control for absorbance measurement).

2. Add 1 ml conc. HCl to each beaker (7) (stir).

3. Add H_2O to bring solution weight to 50.00 g for each beaker.

4. Add 30.0 g of 10% ammonium acetate solution (stir).

5. Add 1.00 g of hydroxylamine hydrochloride solution (stir).

6. Add " " 1,10-phenanthroline " (stir).

7. Add " " pyrocatechol " (stir).

8. Standardize pH meter in 6 to 7 range.

9. Adjust pH of standardization solutions to 6.15 ± 0.05 using either 50% NH_4OH or acetic acid solutions. IF pH goes above 7 during Adjustment, discard solution.

10. Add H_2O to bring total solution weight to 100.0 g for each beaker. Stir 15-25 minutes.

11. Measure absorbances at 585 nm in 10 mm cells. Use control as blank (reference).

12. Plot absorbance vs ppm (linear).

VII. SAMPLE ANALYSIS

1. Tare 250 ml beakers with stirring bars (leave one beaker as a control).

2. Add 10.00 g sample solution into beaker. If the aluminum content is known to exceed 10 ppm, dilute 10X or 100X as needed. If the Al content is below 0.2 ppm, use 50.00 g of sample or longer cells (20, 50 or 100 mm).

3. Add 1 ml conc. HCl to each beaker.

4. Heat sample beakers to 60°C and stir for 1 hour or until solution is complete.

5. Cool to room temperature.

6. Perform steps VI-3 to VI-11.

7. Using calibration chart prepared in step VI-12, read ppm in sample solution.

VIII. REFERENCE

CD&P Method W200.015

LA/kkg

XIII. INDEXING TERMS

Surface alumina on TiO_2 pigments

Restructuring of surface alumina on TiO_2 pigments

TiO_2 pigment colloidal properties

Aluminum adsorption/desorption by TiO_2 pigments

Measurement of soluble aluminum

Flocculation behavior of TiO_2 pigments

Tamol 731 adsorption by TiO_2 pigments

Effect of pH on Tamol 731 adsorption

Reactor discharge slurry

Pigment surface chemistry

Adsorption measurements on TiO_2 pigments

Zeta potential measurements of TiO_2 pigment suspensions

Size measurements of TiO_2 pigment suspensions

Humate flocculation

Competitive TiO_2 pigments

Figure 1. Shift in Z.P. of R-900 Cyclone Discharge

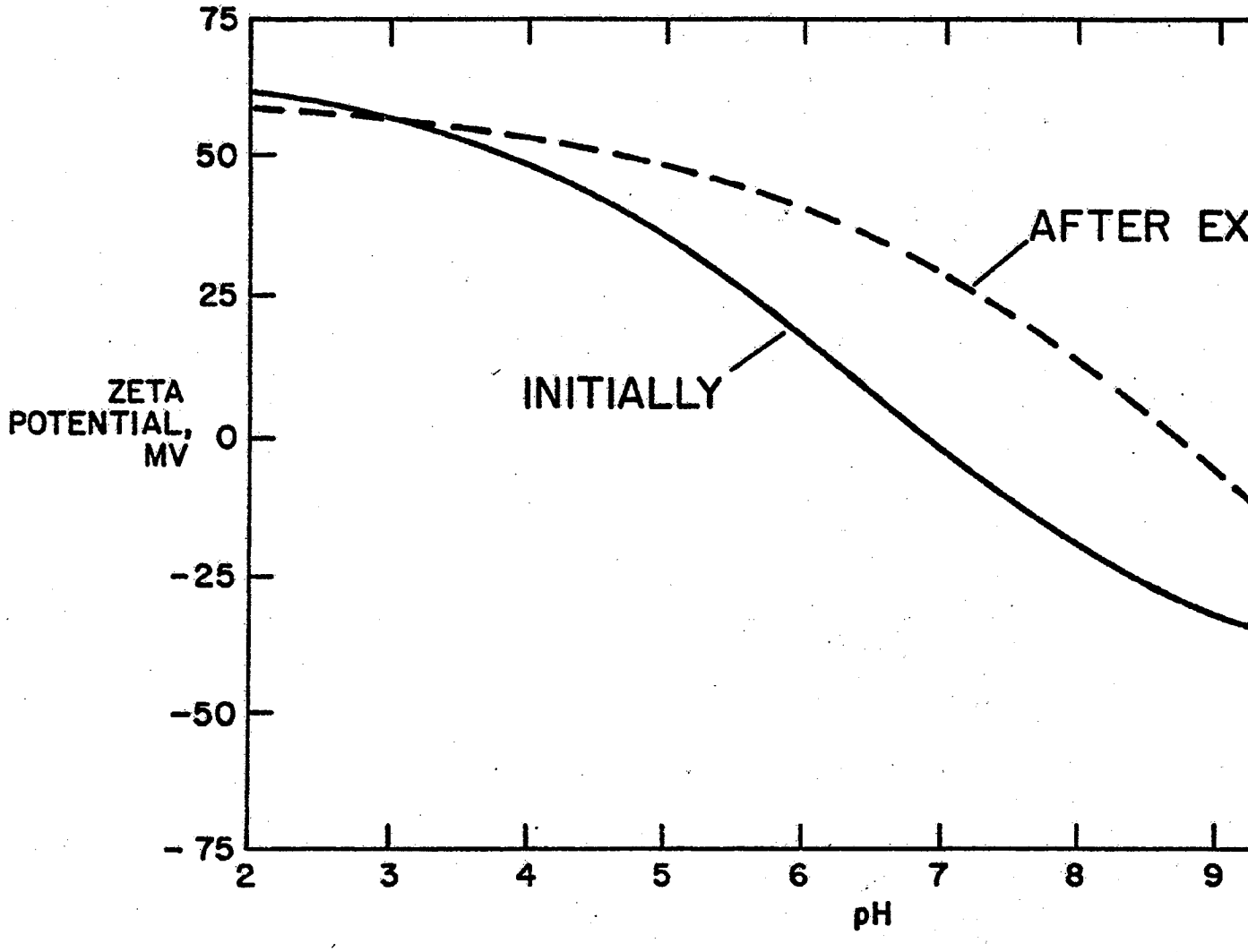

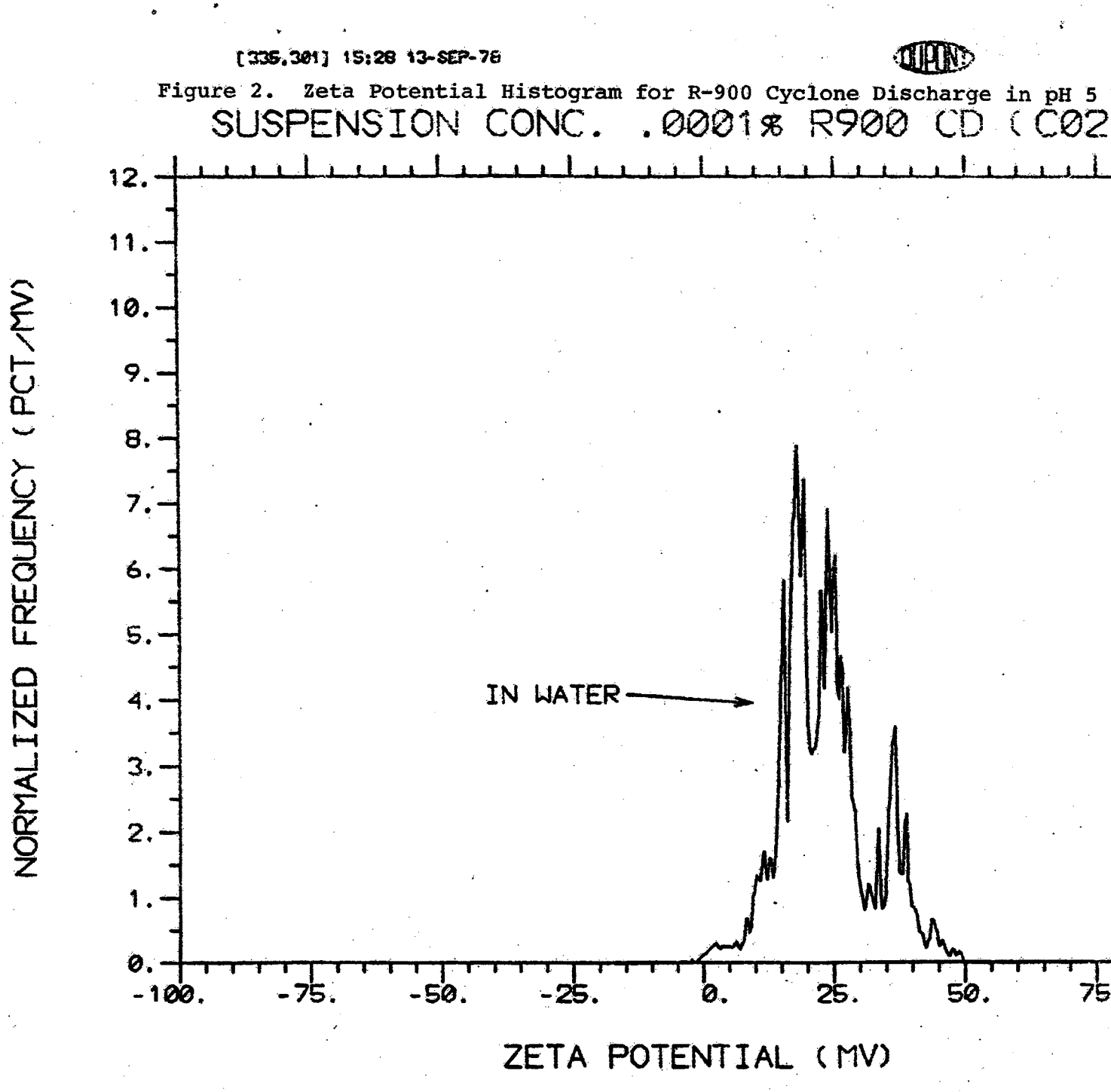

Figure 2. Zeta Potential Histogram for R-900 Cyclone Discharge in pH 5

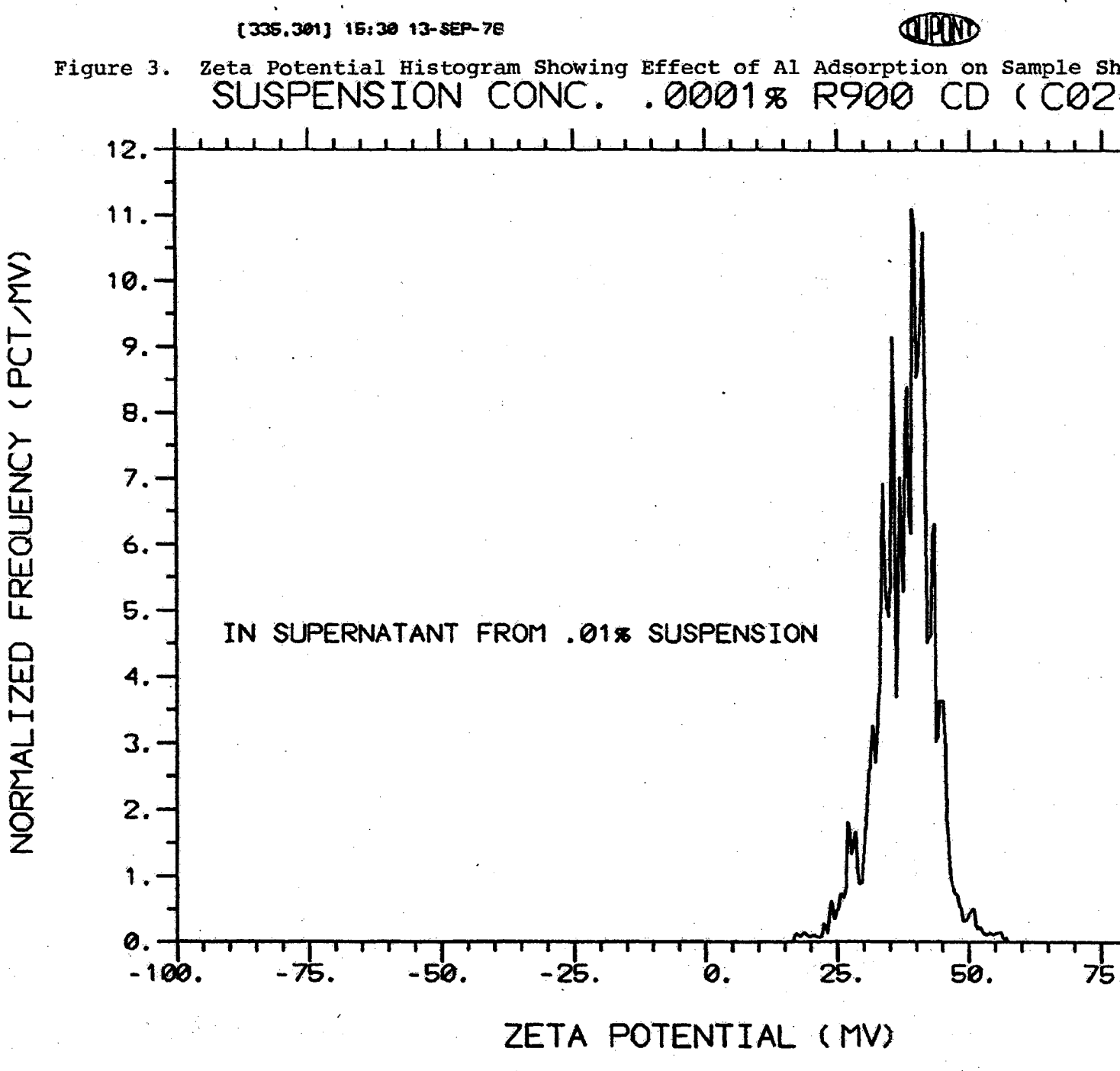

Figure 3. Zeta Potential Histogram Showing Effect of Al Adsorption on Sample Sh

Figure 4. Zeta Potential Measurements for 'Cleaned' R-900 C.D.

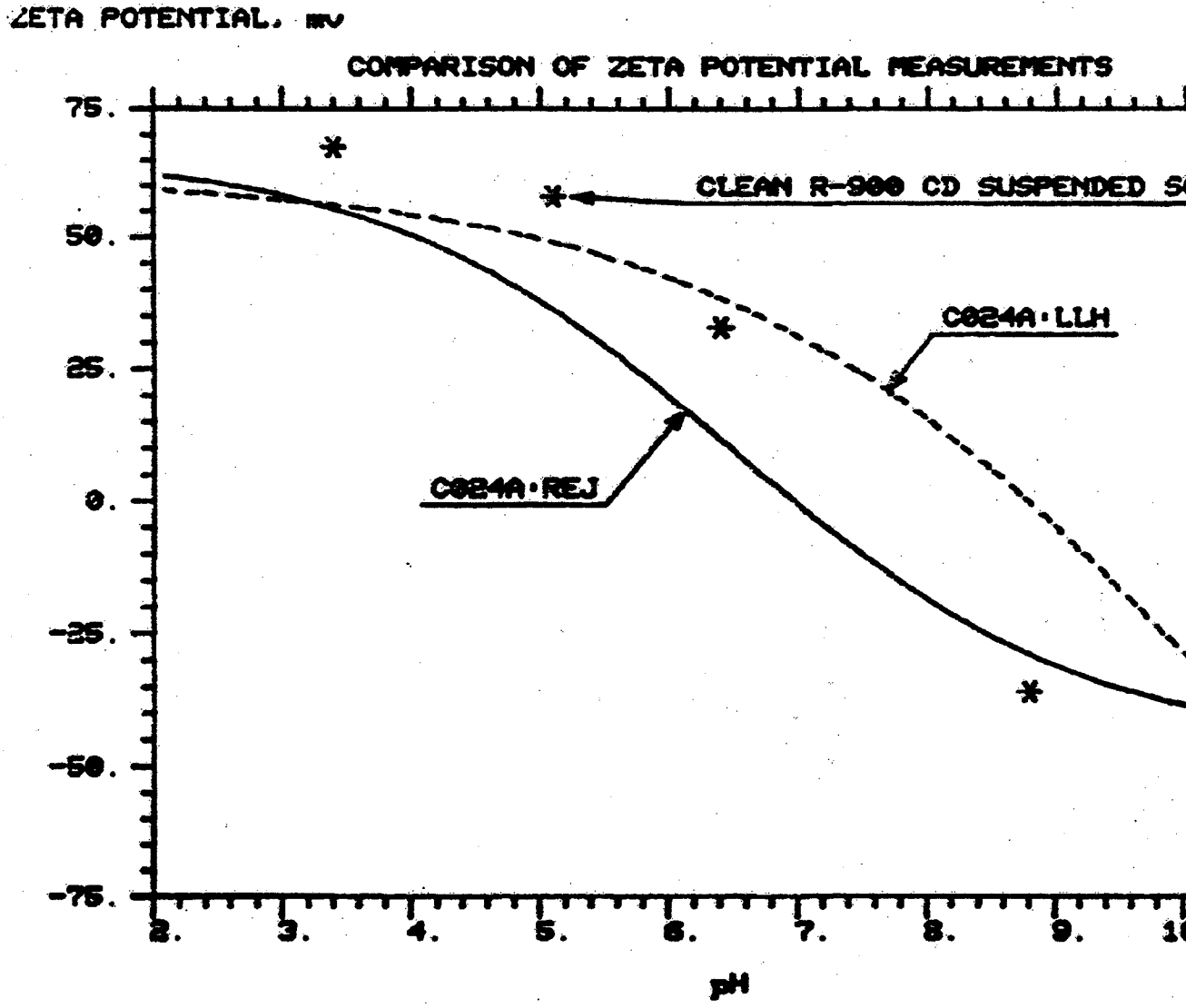

Figure 5
EFFECT OF pH ON ZETA POTENTIAL HISTOGRAM OF
CLEAN R-900 (CD)

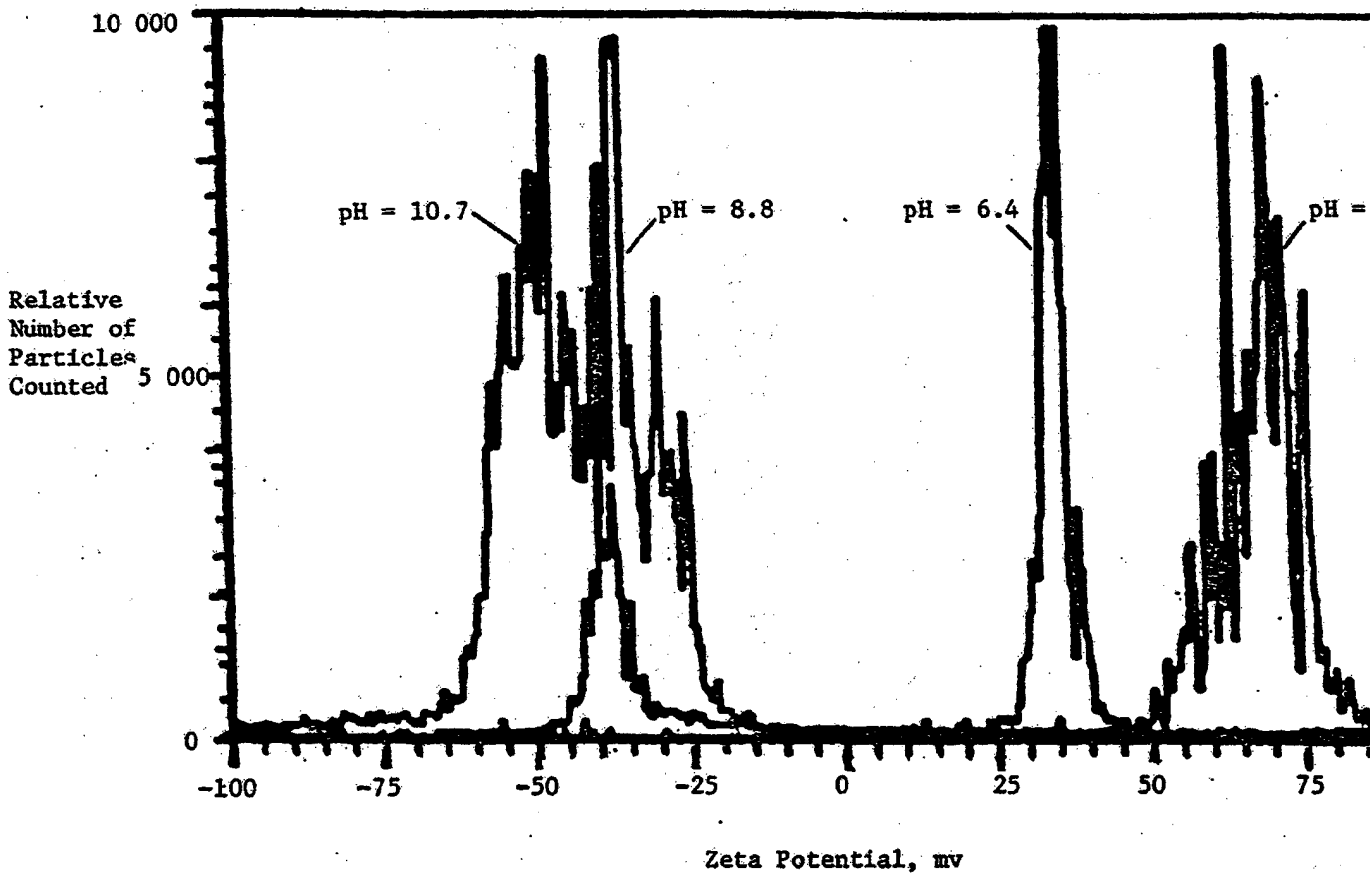

Figure 6. Calibration Curve for Measuring Soluble Aluminum

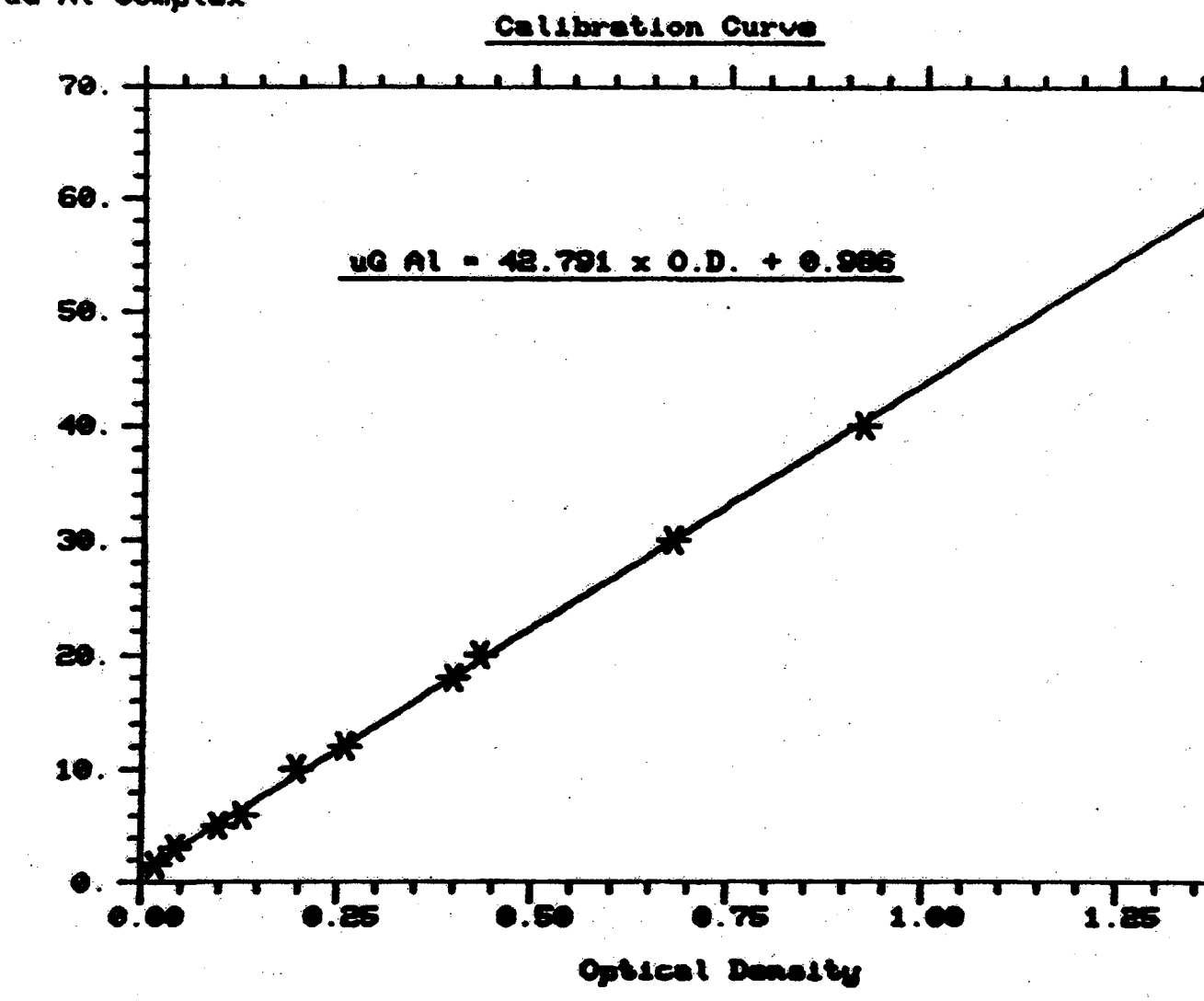

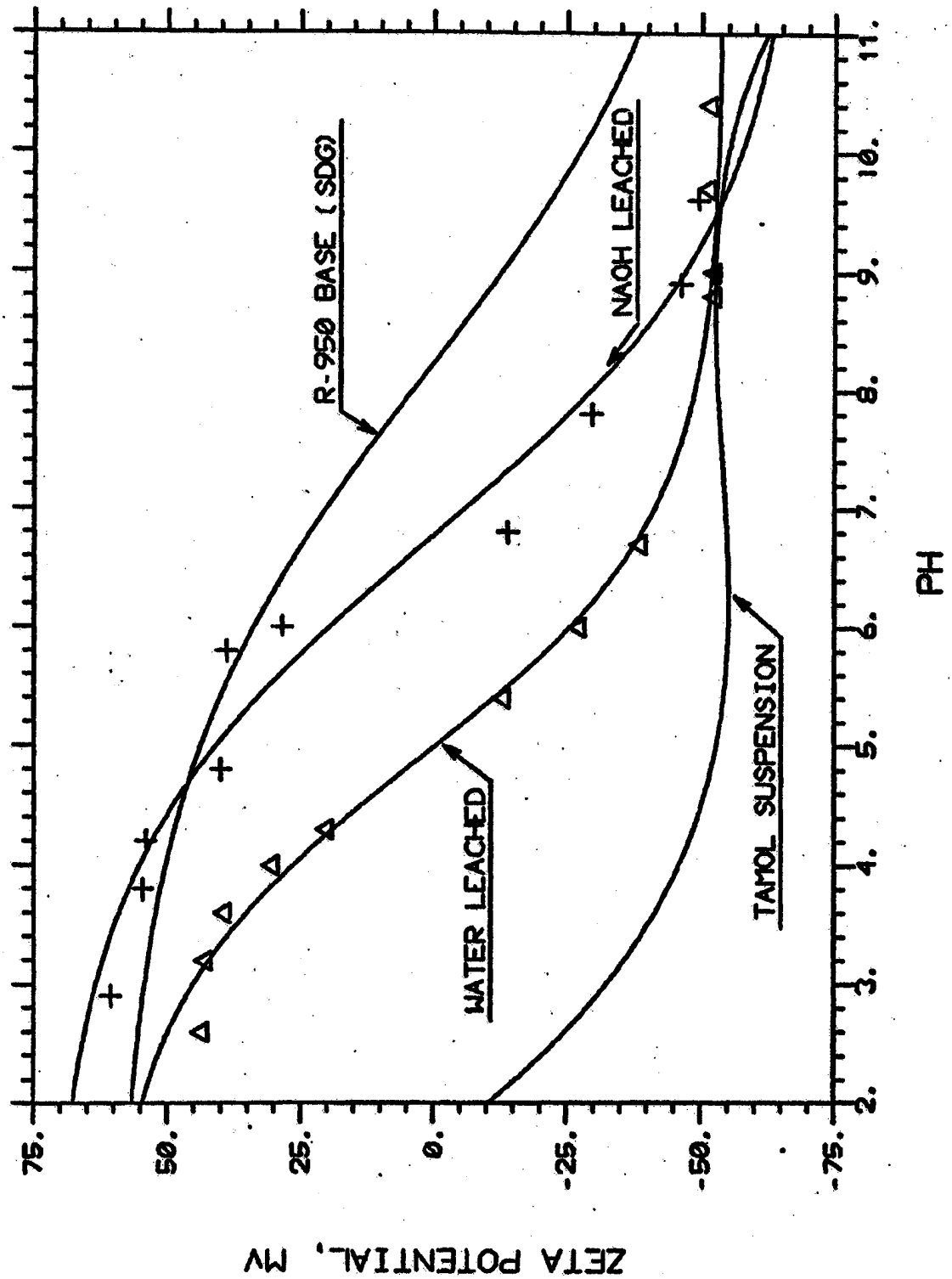

Figure 7. Zeta Potential-pH Curves for TiO_2 Recovered from R-950

Figure 8. Transient Turbidity Sizes for R-900 and R-960 Aqueous/Tamol Suspe

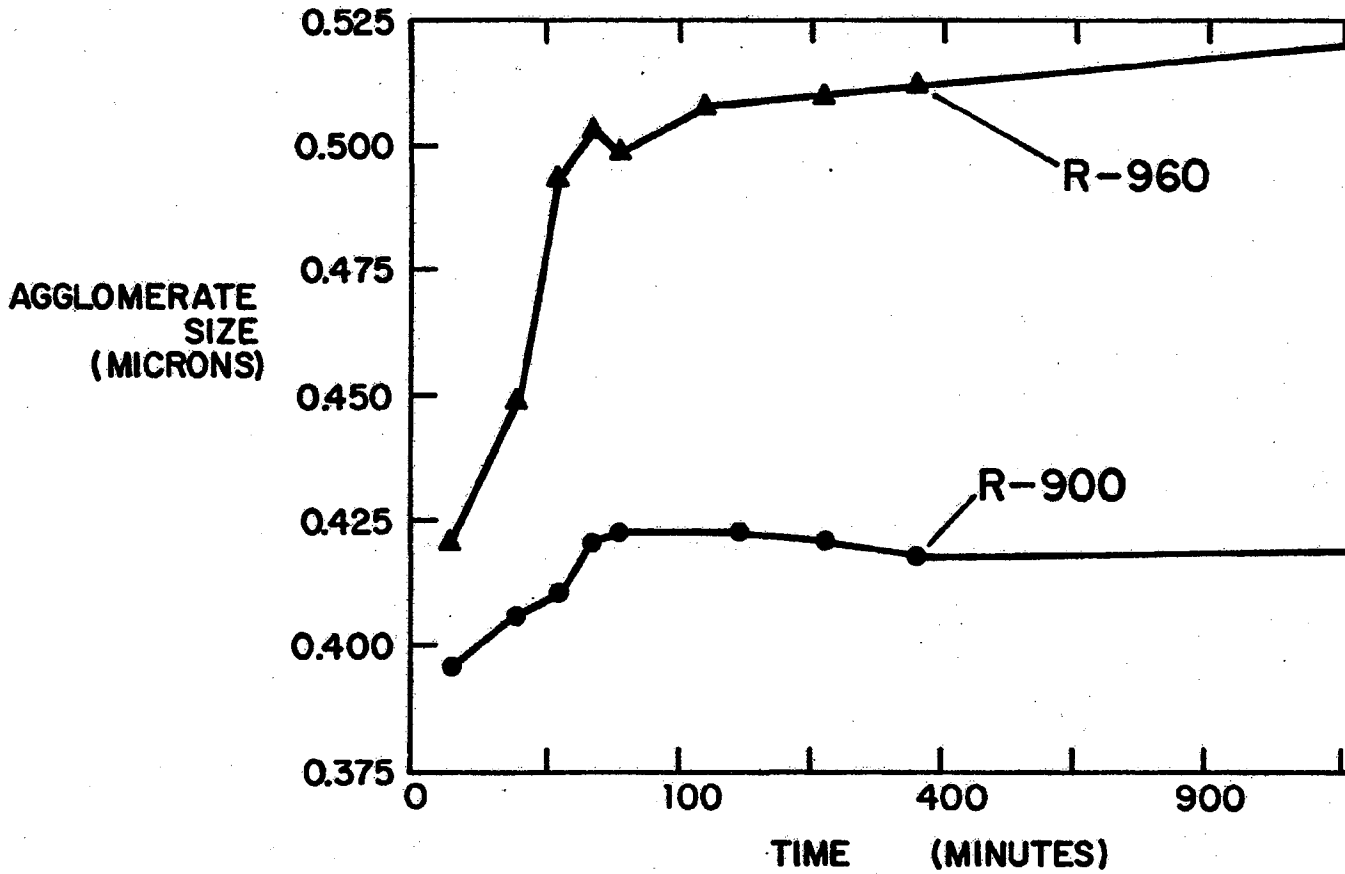

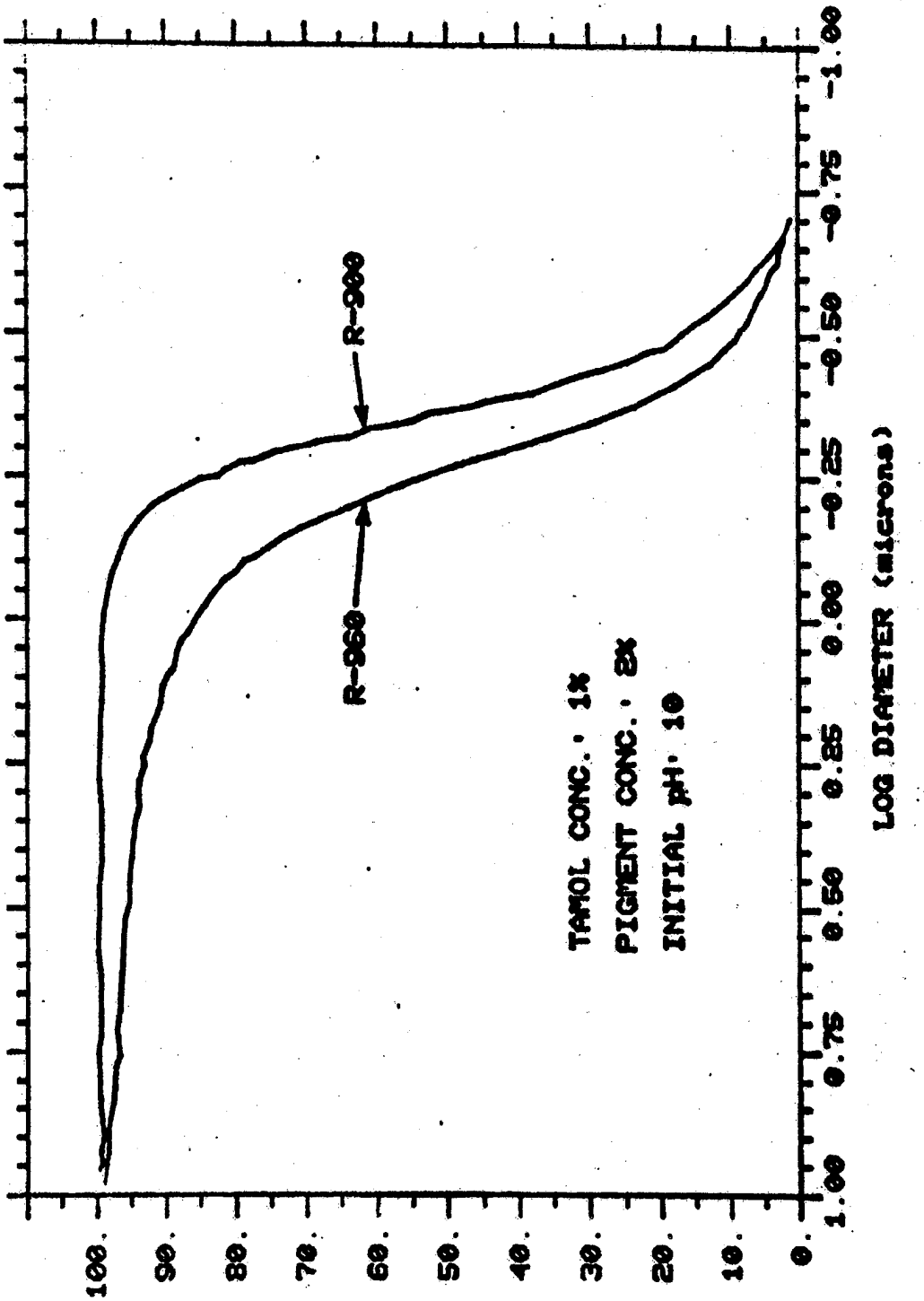

Figure 9. Sedigraph Particle Size Distributions for R-900 and R-960 Aqueous/Tamol Suspensions

Figure 10. Transient Turbidity Sizes for R-900 and Two Lab Alumina-Coated

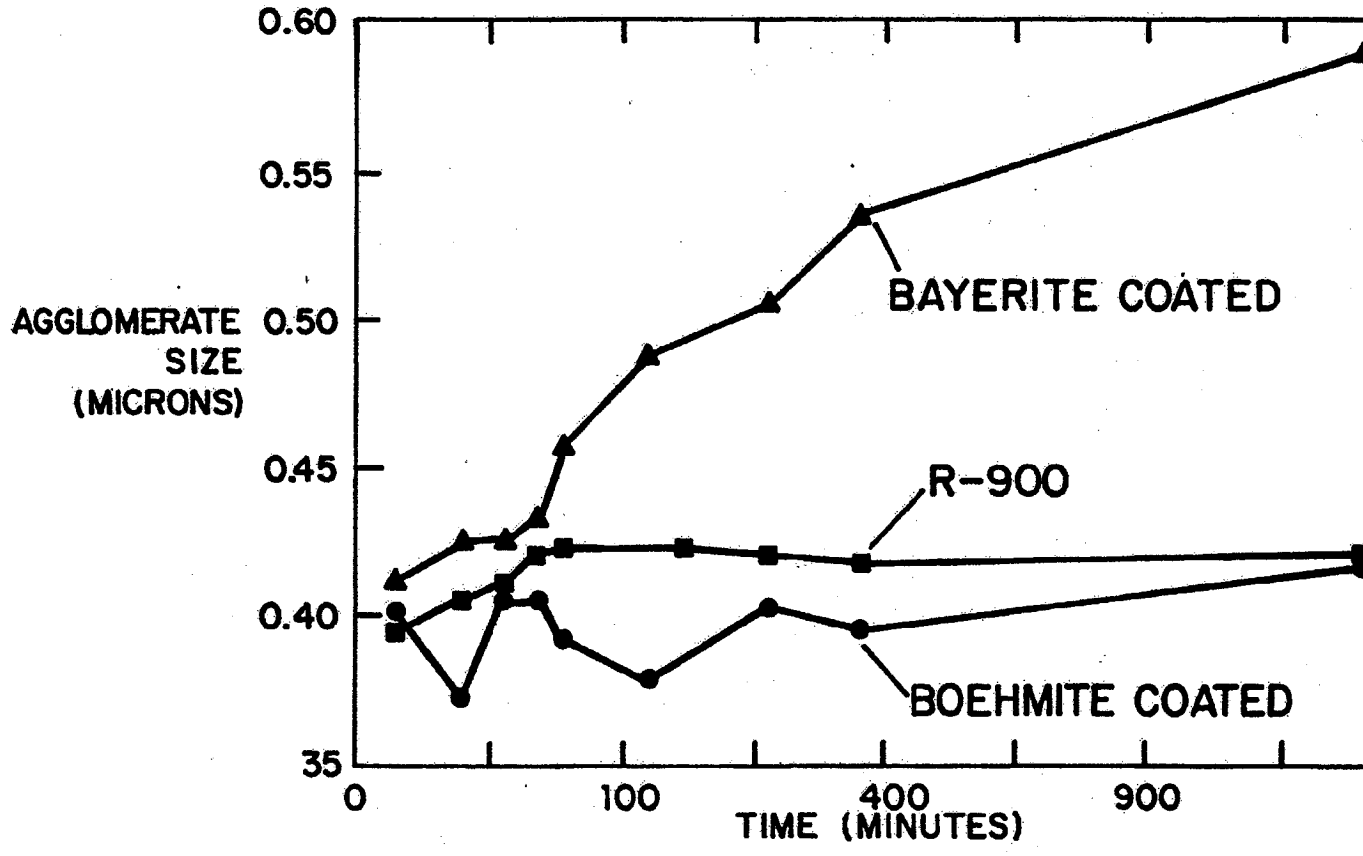

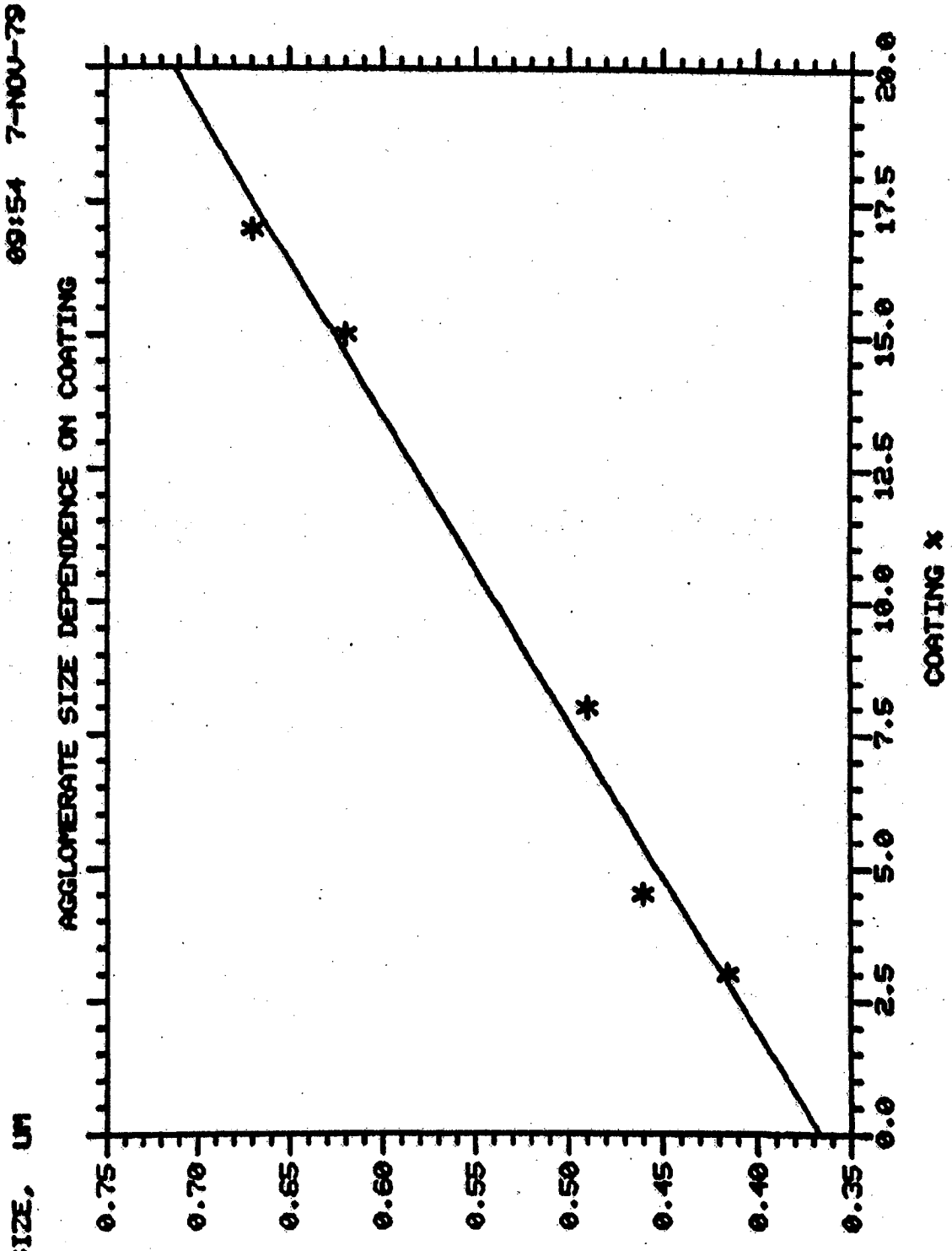

Figure 11. Dependence of Agglomerate Size on Amount of Hydrous Oxide Coating

Figure 12

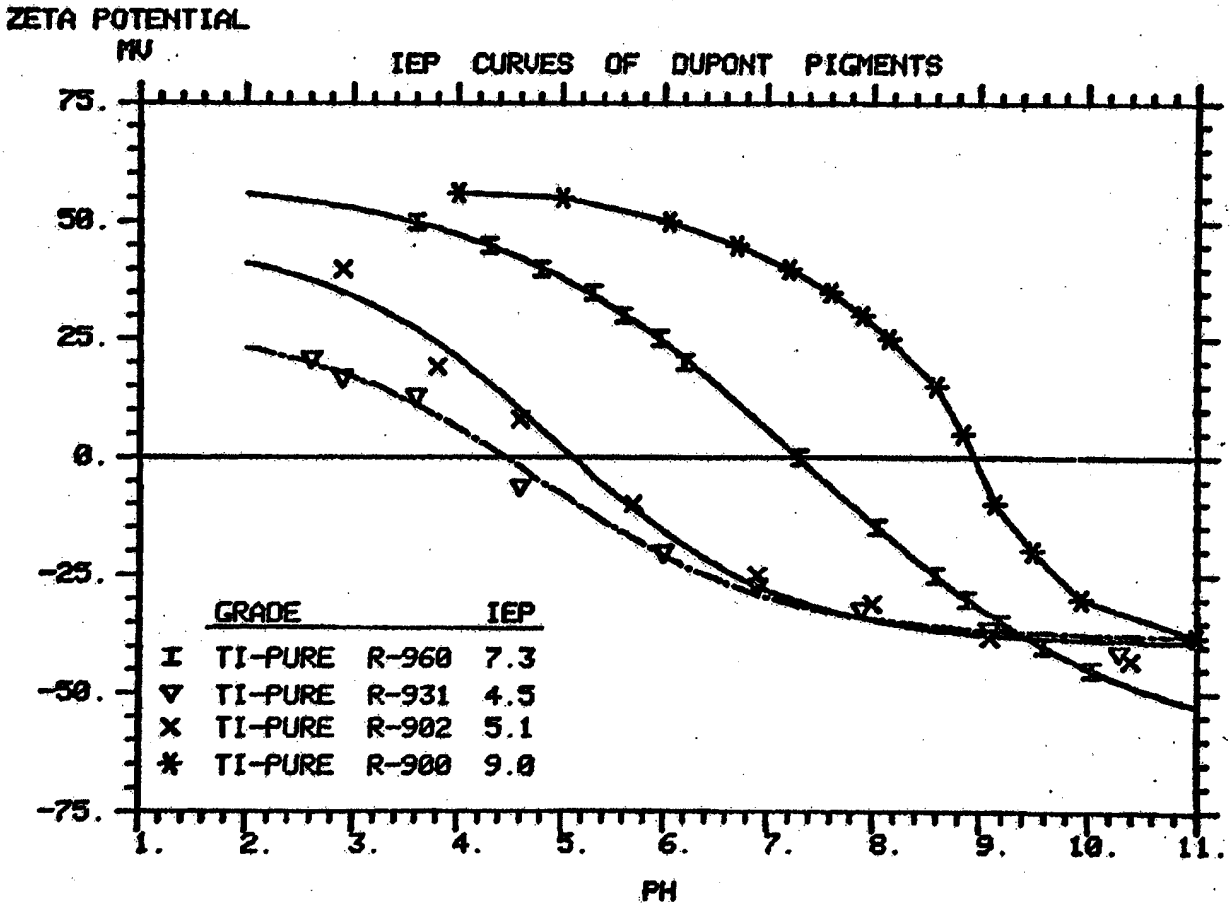
ZETA POTENTIAL
MV
IEP CURVES OF DUPONT PIGMENTS
75.
50.
25.
0.
-25.
-50.
-75.
1.
2.
3.
4.
5.
6.
7.
8.
9.
10.
11.
PH
GRADE IEP
TI-PURE R-960 7.3
TI-PURE R-931 4.5
TI-PURE R-902 5.1
TI-PURE R-900 9.0

Figure 13

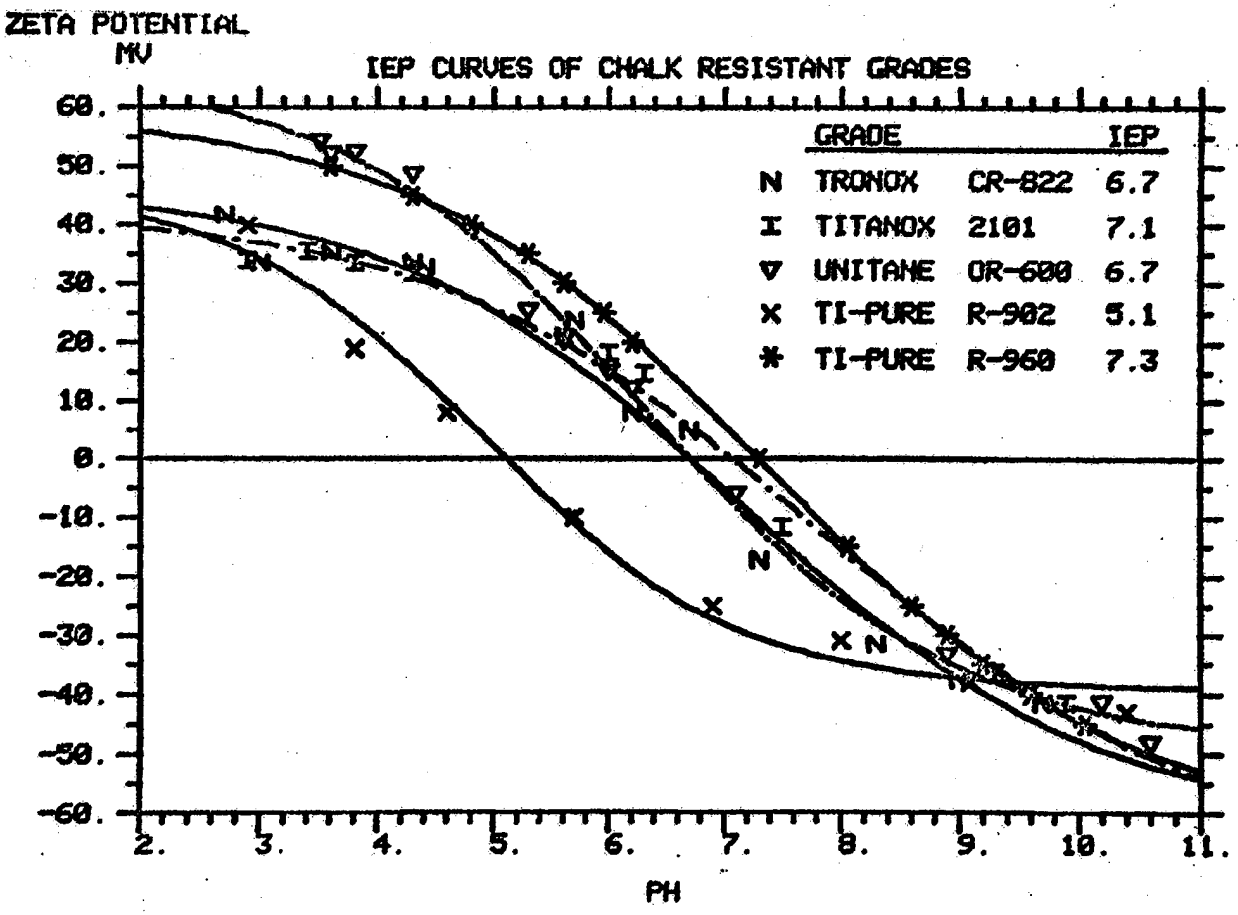

Figure 14

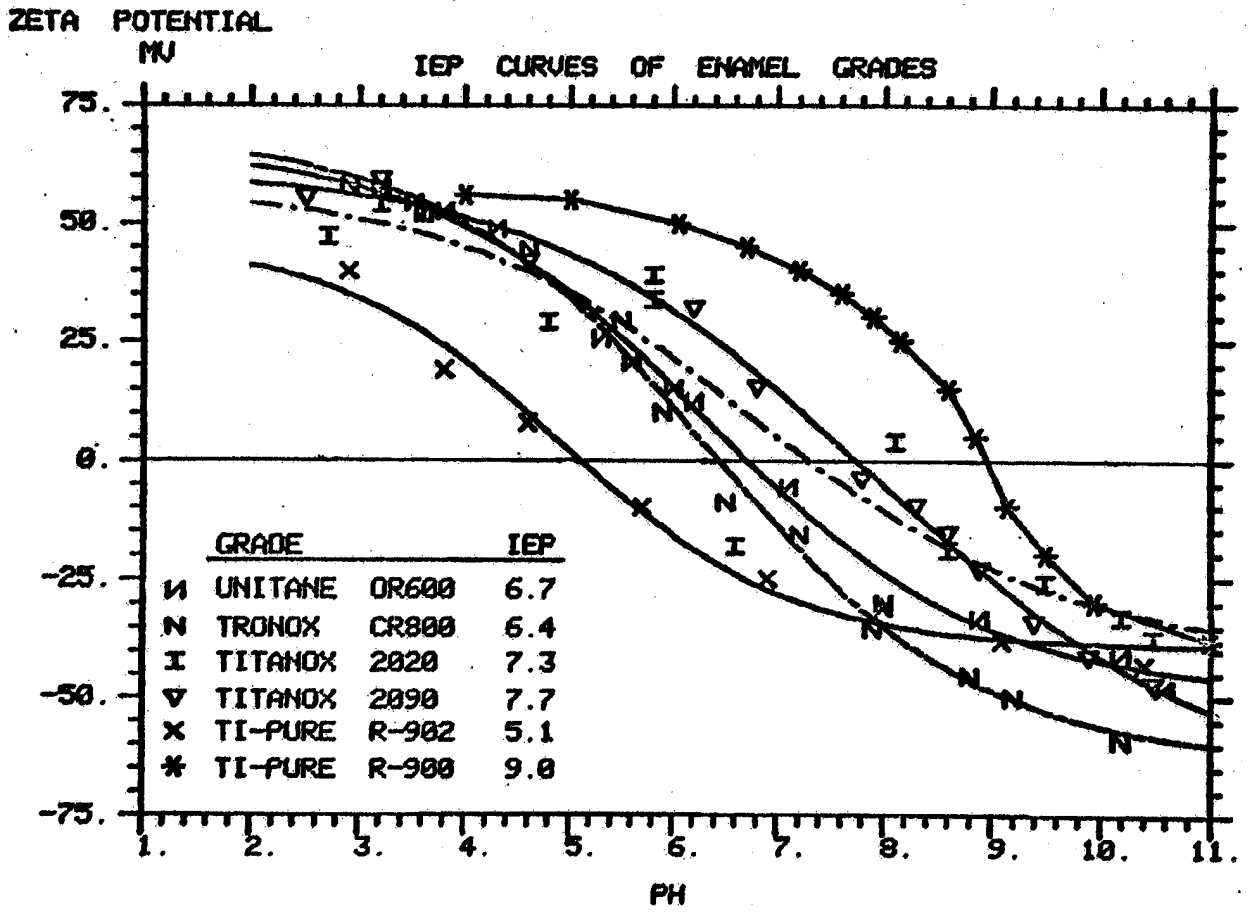

Figure 15

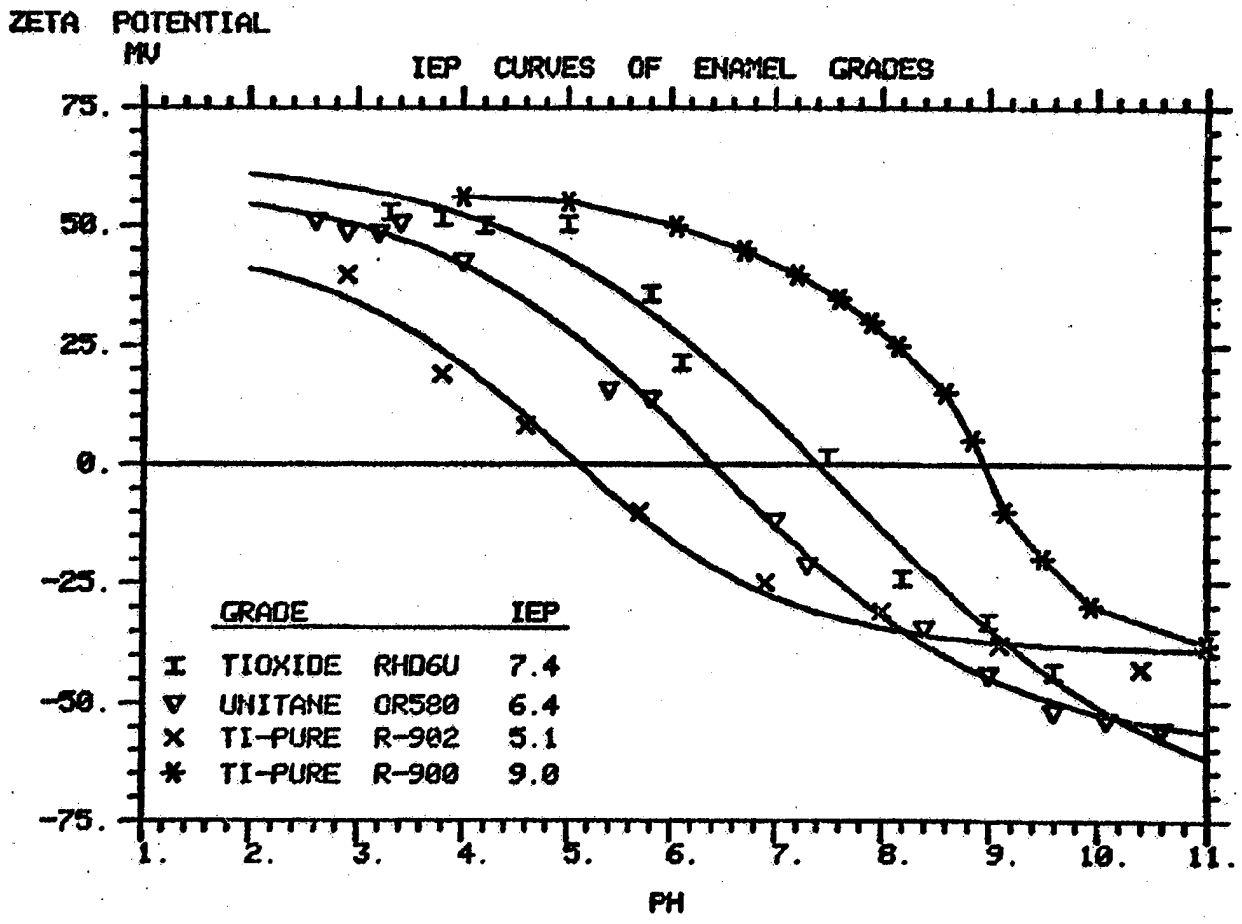

Figure 16

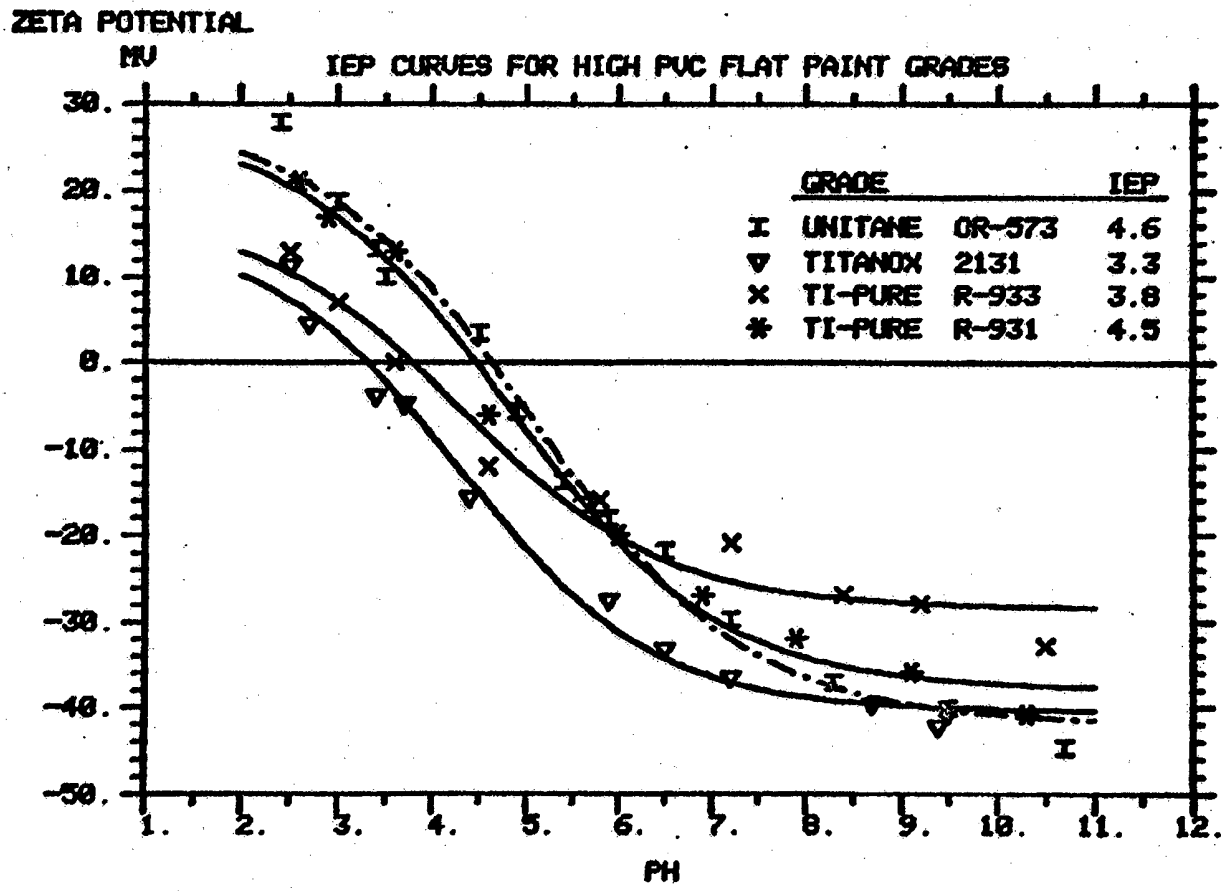

Figure 17

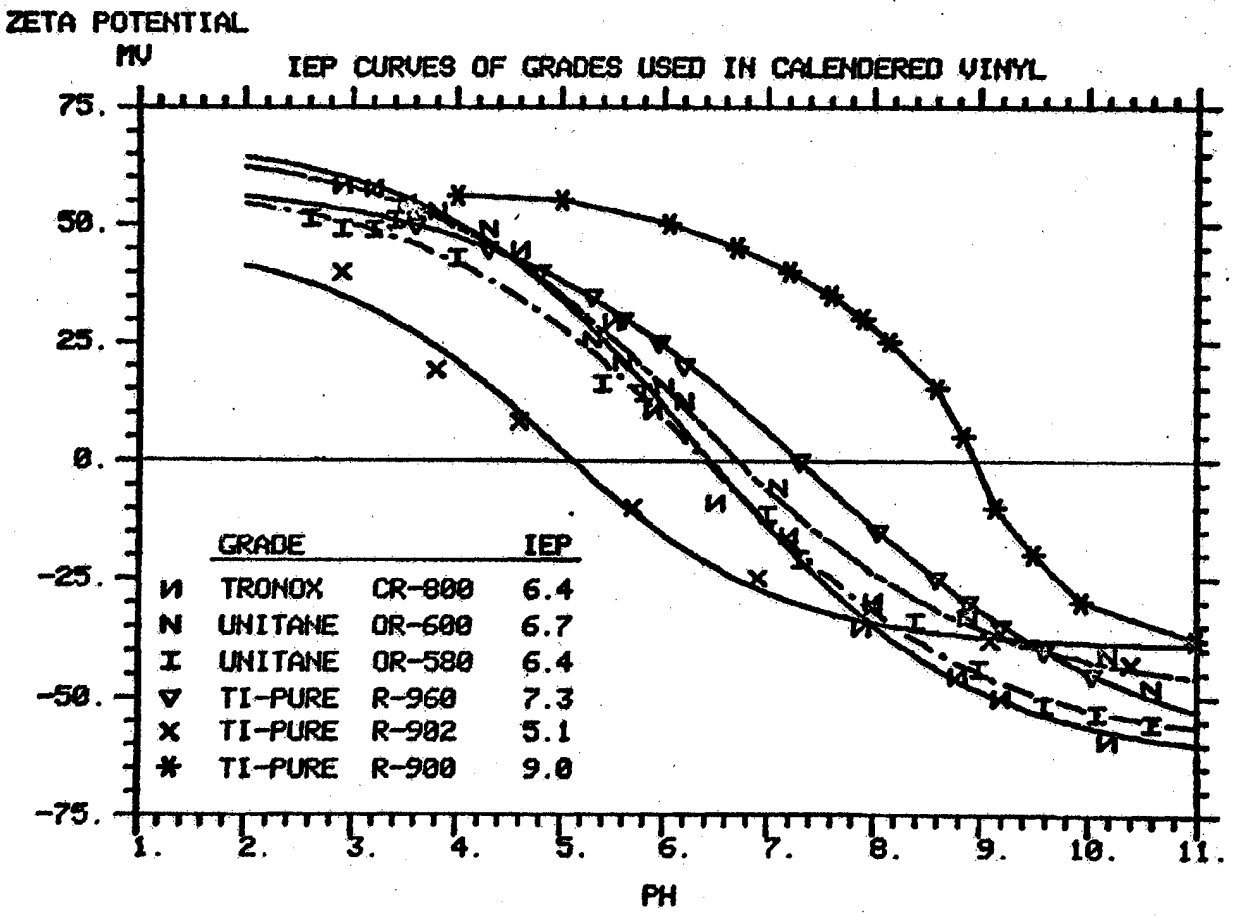
ZETA POTENTIAL
MV
IEP CURVES OF GRADES USED IN CALENDERED VINYL
75.
50.
25.
0.
-25.
-50.
-75.
1.
2.
3.
4.
5.
6.
7.
8.
9.
10.
11.
PH
GRADE
IEP
M TRONOX CR-800 6.4
N UNITANE OR-600 6.7
I UNITANE OR-580 6.4
▽ TI-PURE R-960 7.3
X TI-PURE R-902 5.1
* TI-PURE R-900 9.0

Figure 18

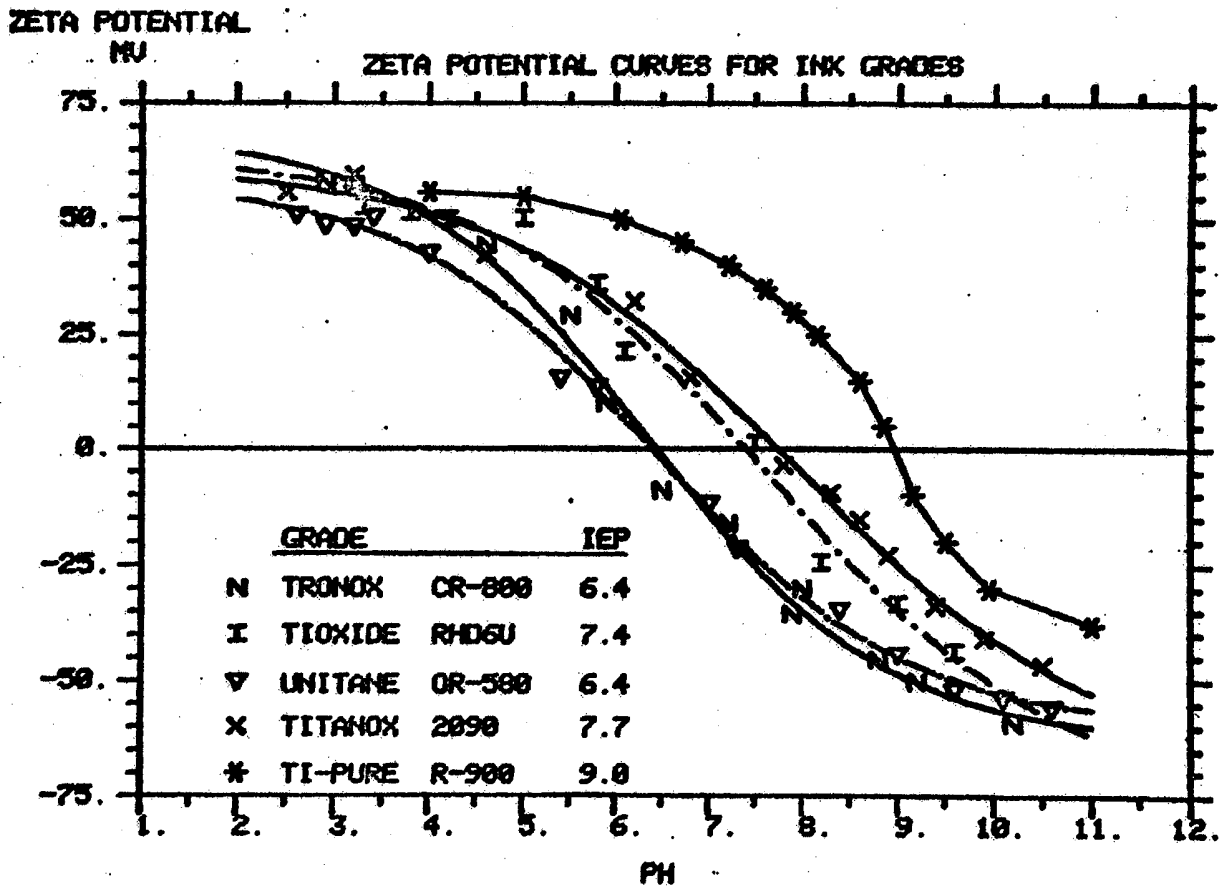

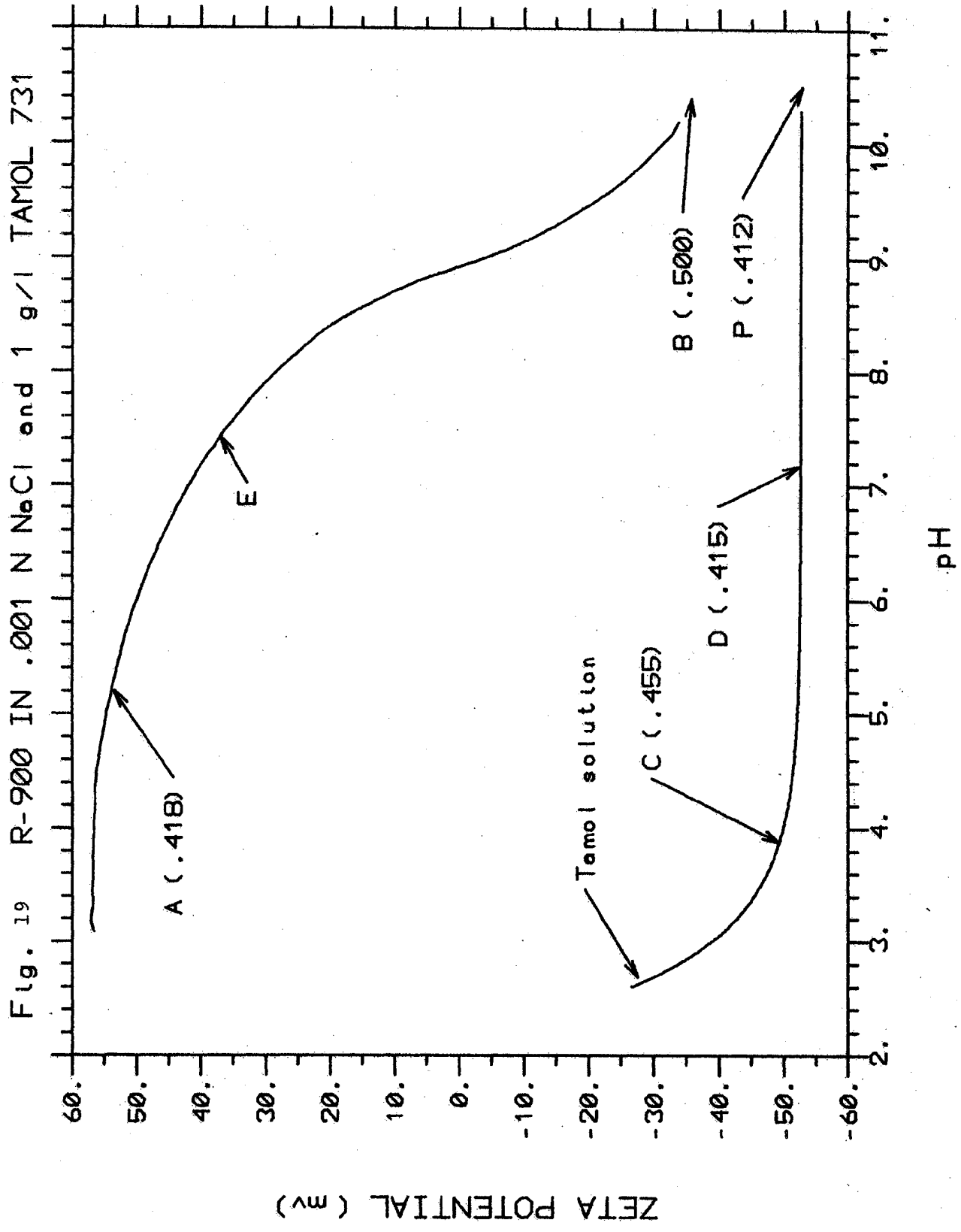

Fig. 20 R-960 IN .001 N NaCl and 1 g/l TAMOL

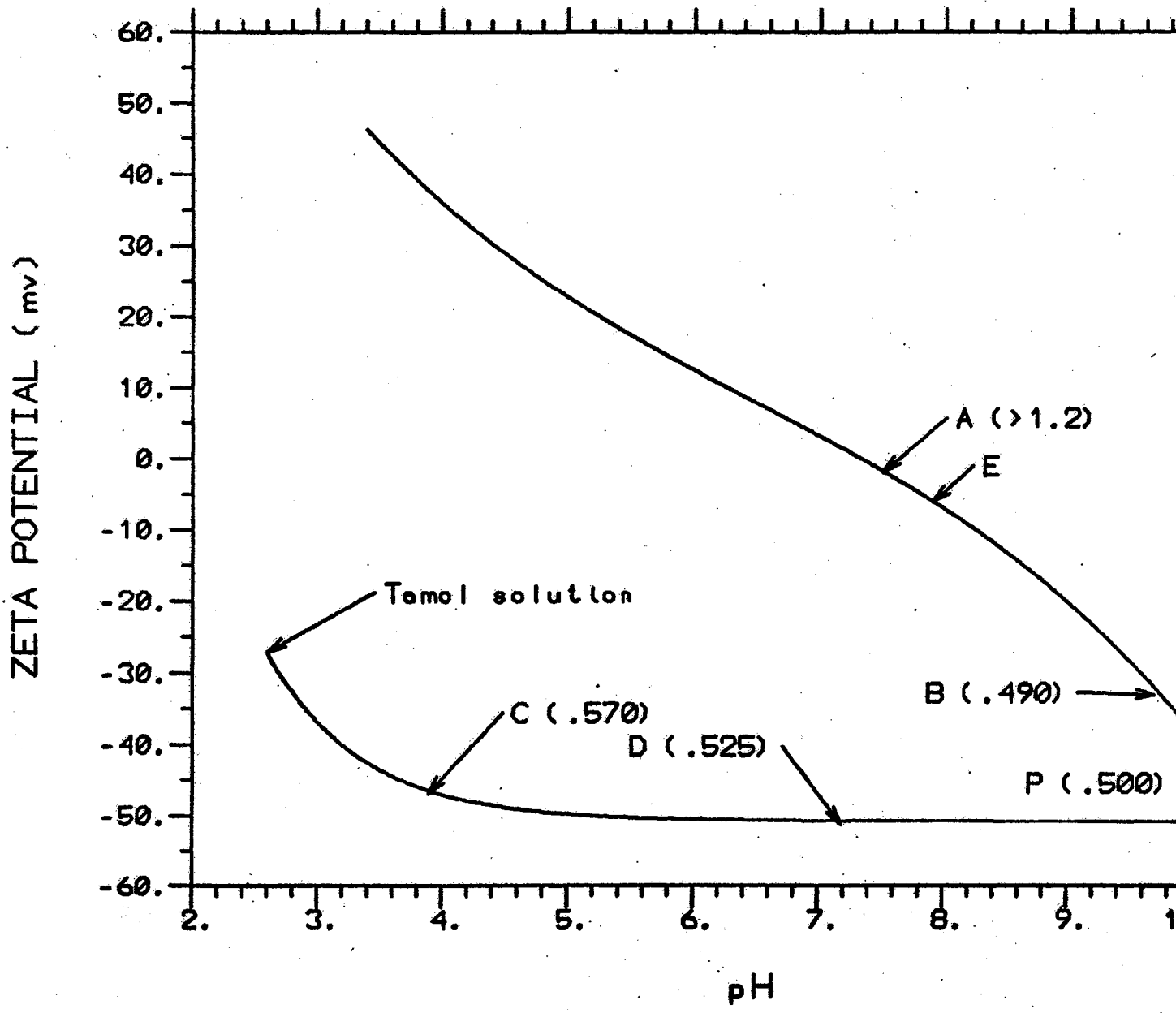

Figure 21

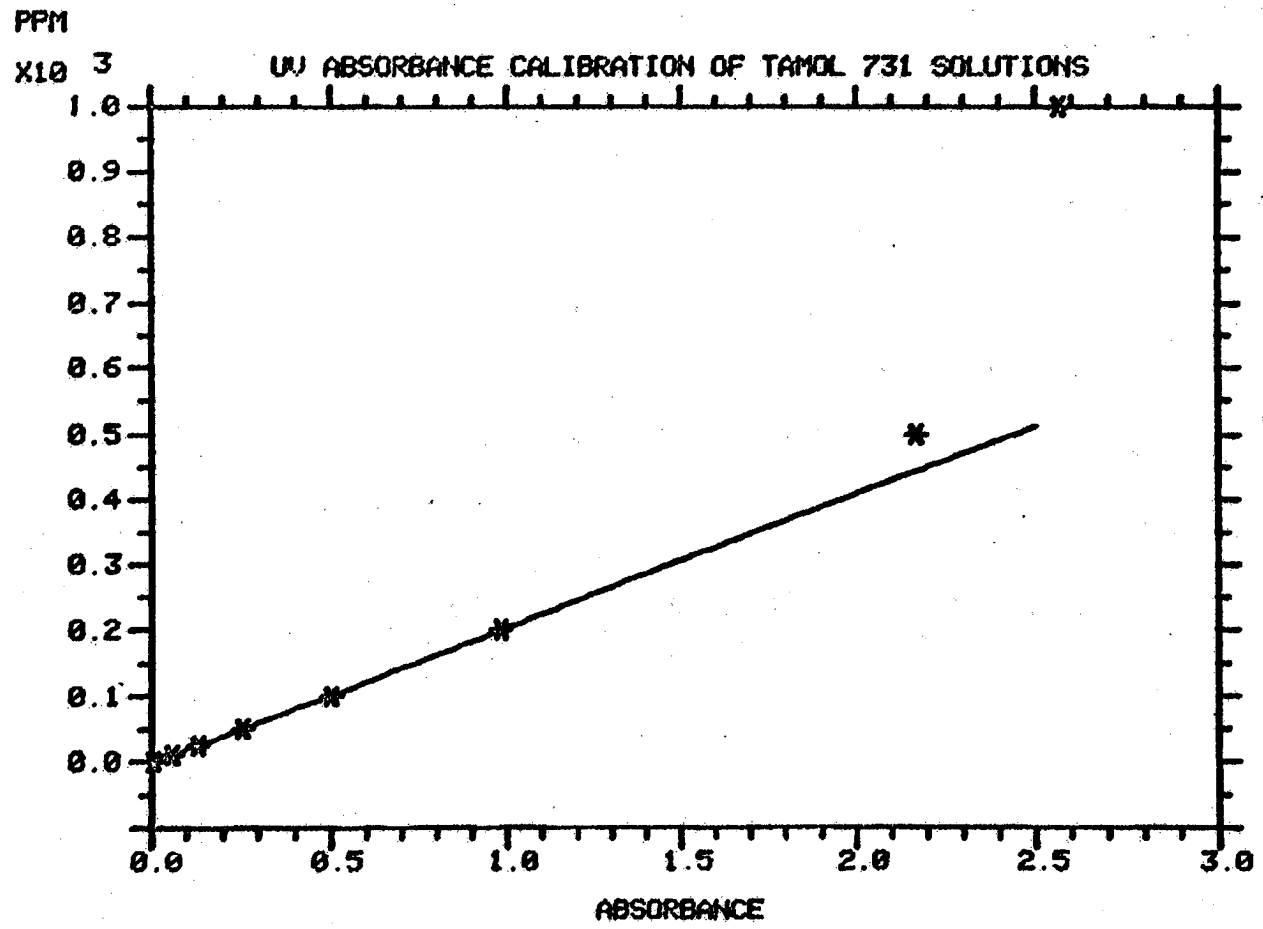
PPM
X10 3
UV ABSORBANCE CALIBRATION OF TAMOL 731 SOLUTIONS
1.0
0.9
0.8
0.7
0.6
0.5
0.4
0.3
0.2
0.1
0.0
0.0
0.5
1.0
1.5
2.0
2.5
3.0
ABSORBANCE

Figure 22

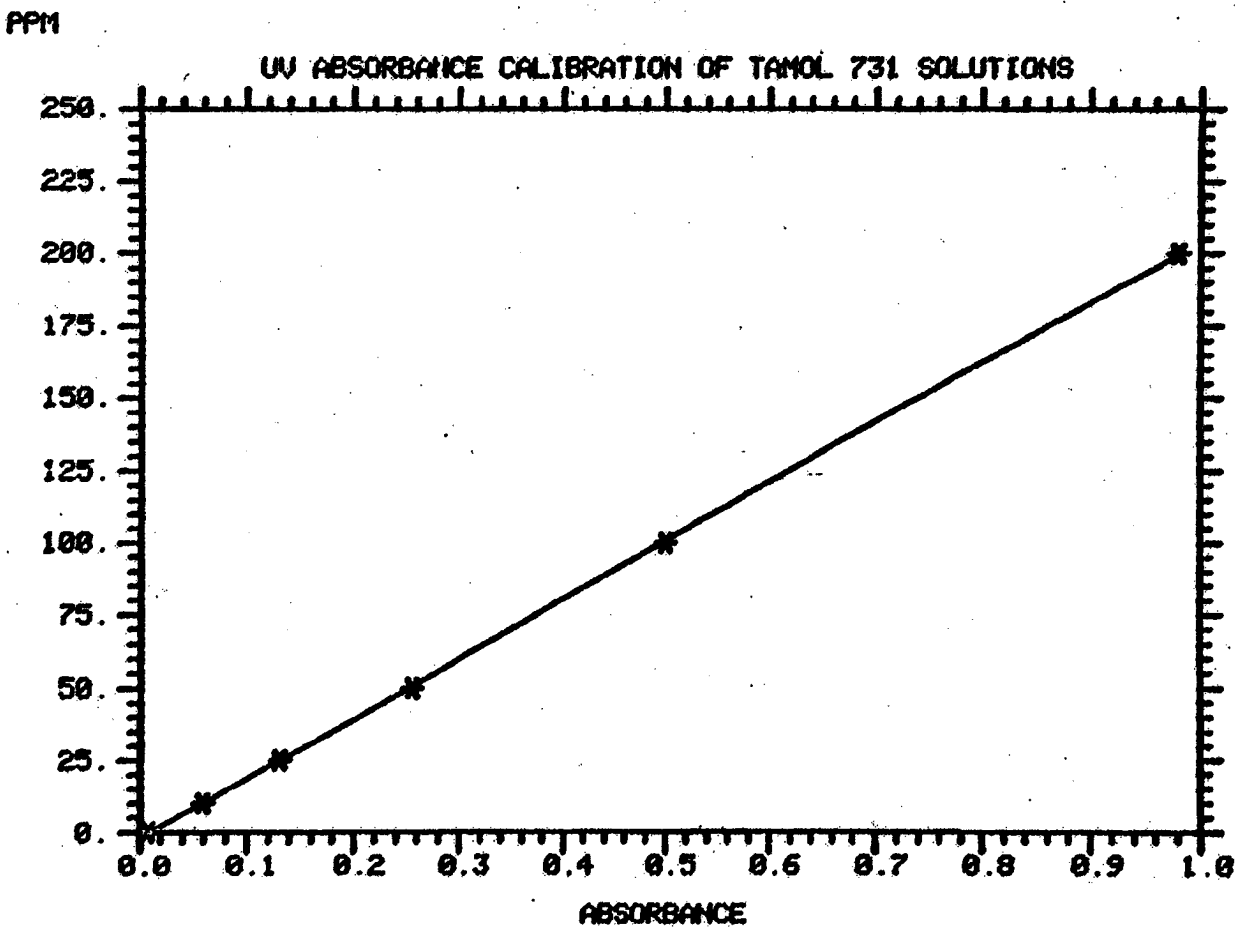
PPM
UV ABSORBANCE CALIBRATION OF TAMOL 731 SOLUTIONS
250.
225.
200.
175.
150.
125.
100.
75.
50.
25.
0.
0.0
0.1
0.2
0.3
0.4
0.5
0.6
0.7
0.8
0.9
1.0
ABSORBANCE

Figure 23

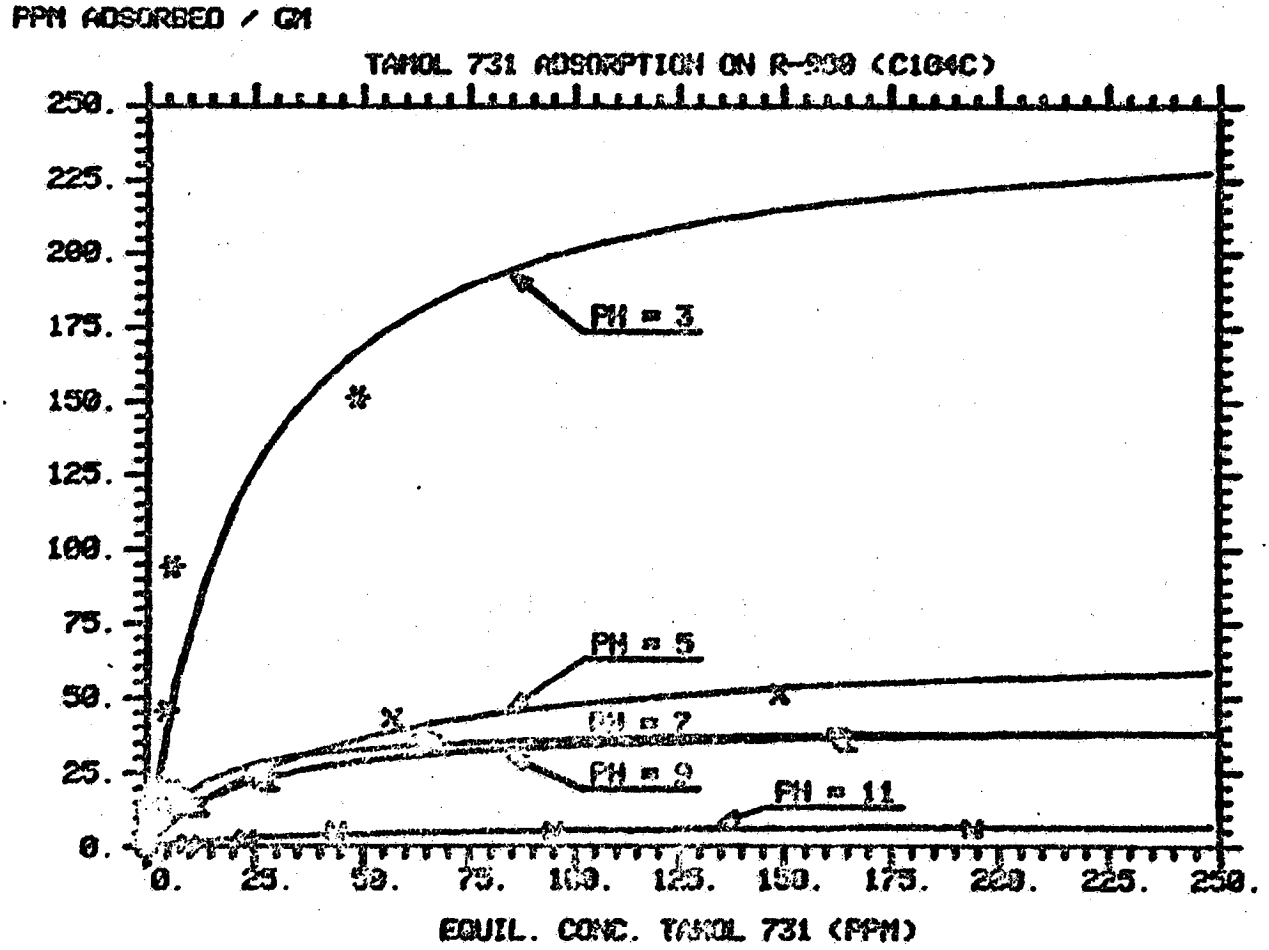
PPM ADSORBED / GM
TAMOL 731 ADSORPTION ON R-930 (C104C)
250.
225.
200.
175.
150.
125.
100.
75.
50.
25.
0.
PH = 3
PH = 5
PH = 7
PH = 9
PH = 11
0.
25.
50.
75.
100.
125.
150.
175.
200.
225.
250.
EQUIL. CONC. TAMOL 731 (PPM)

Figure 24

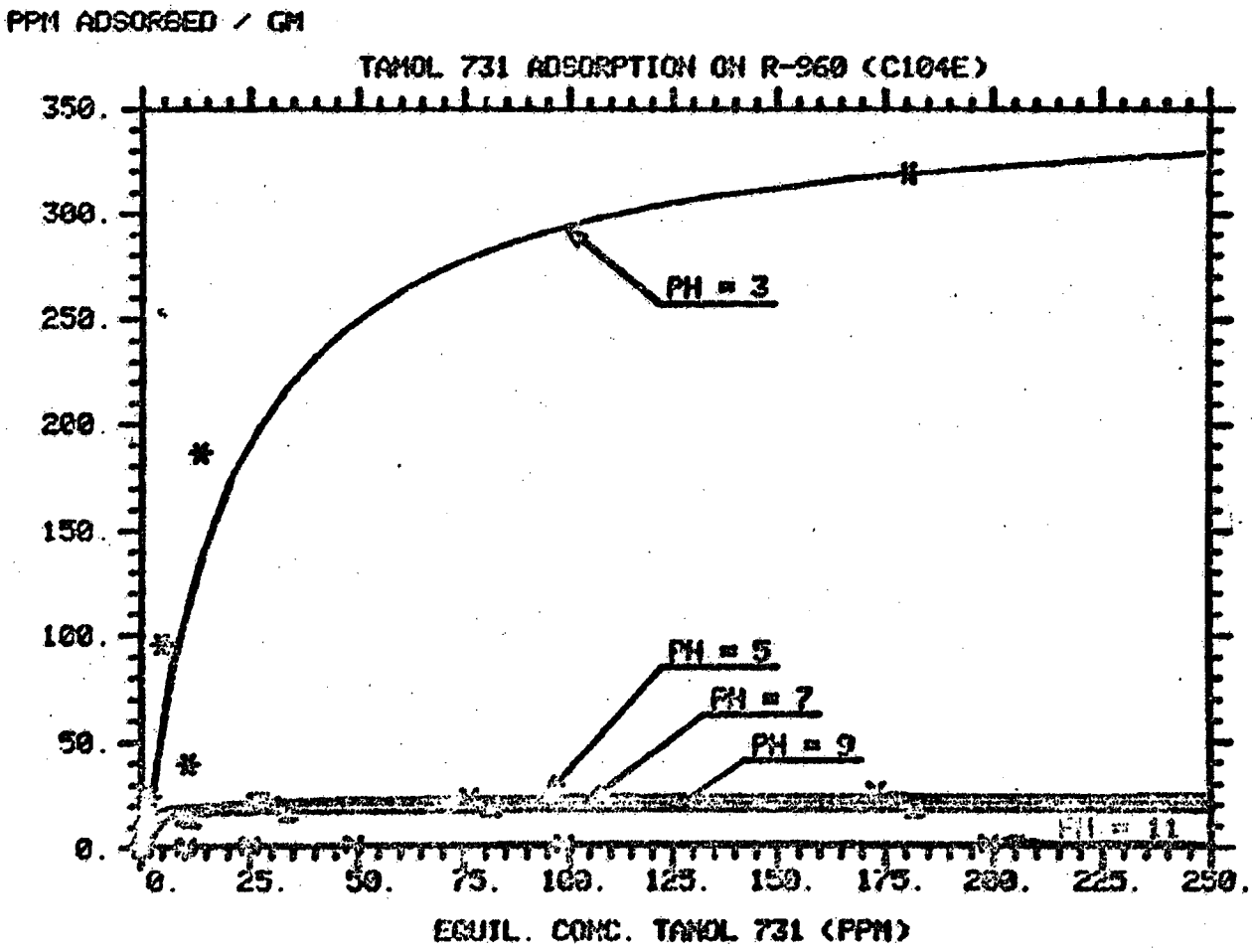
PPM ADSORBED / GM
TAMOL 731 ADSORPTION ON R-960 (C104E)
350.
300.
250.
200.
150.
100.
50.
0.
PH = 3
PH = 5
PH = 7
PH = 9
PH = 11
0.
25.
50.
75.
100.
125.
150.
175.
200.
225.
250.
EQUIL. CONC. TAMOL 731 (PPM)

Figure 25

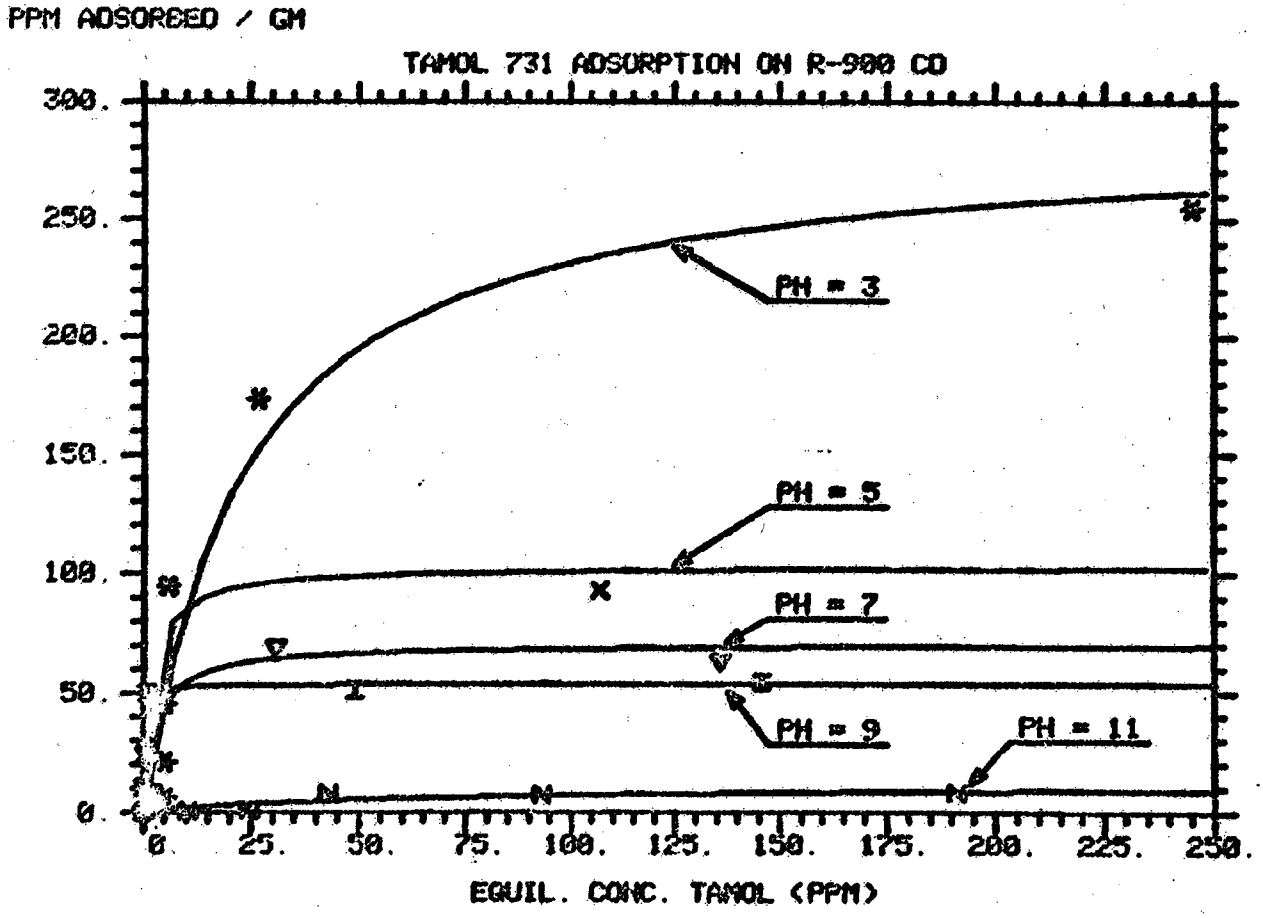
PPM ADSORBED / GM
TAMOL 731 ADSORPTION ON R-900 CO
300.
250.
200.
150.
100.
50.
0.
PH = 3
PH = 5
PH = 7
PH = 9
PH = 11
0.
25.
50.
75.
100.
125.
150.
175.
200.
225.
250.
EQUIL. CONC. TAMOL (PPM)

Figure 26

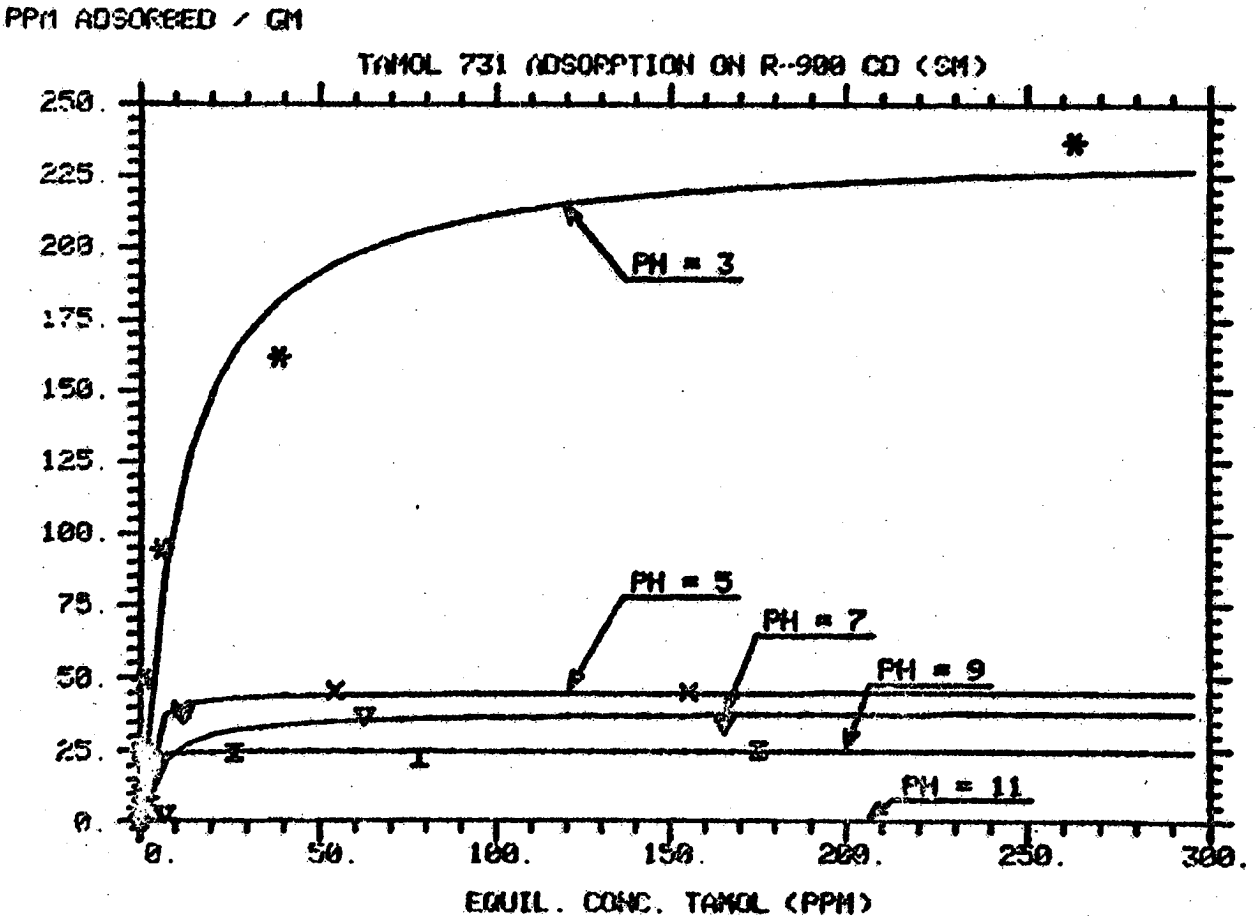
PPM ADSORBED / GM
TAMOL 731 ADSORPTION ON R-900 CO (3M)
250.
225.
200.
175.
150.
125.
100.
75.
50.
25.
0.
PH = 3
PH = 5
PH = 7
PH = 9
PH = 11
0.
50.
100.
150.
200.
250.
300.
EQUIL. CONC. TAMOL (PPM)

Figure 27

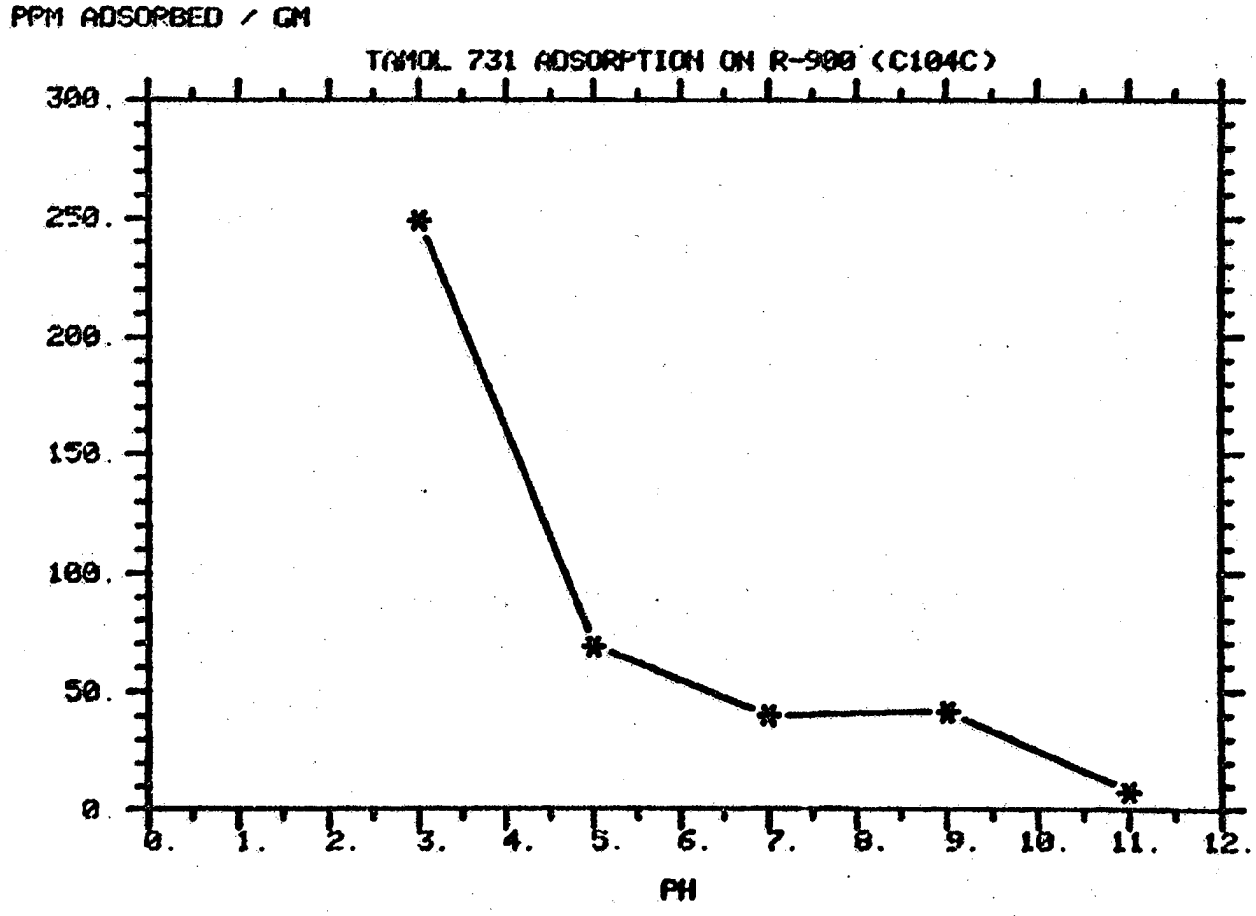
PPM ADSORBED / GM
TAMOL 731 ADSORPTION ON R-900 (C104C)
300.
250.
200.
150.
100.
50.
0.
0.
1.
2.
3.
4.
5.
6.
7.
8.
9.
10.
11.
12.
PH

Figure 28

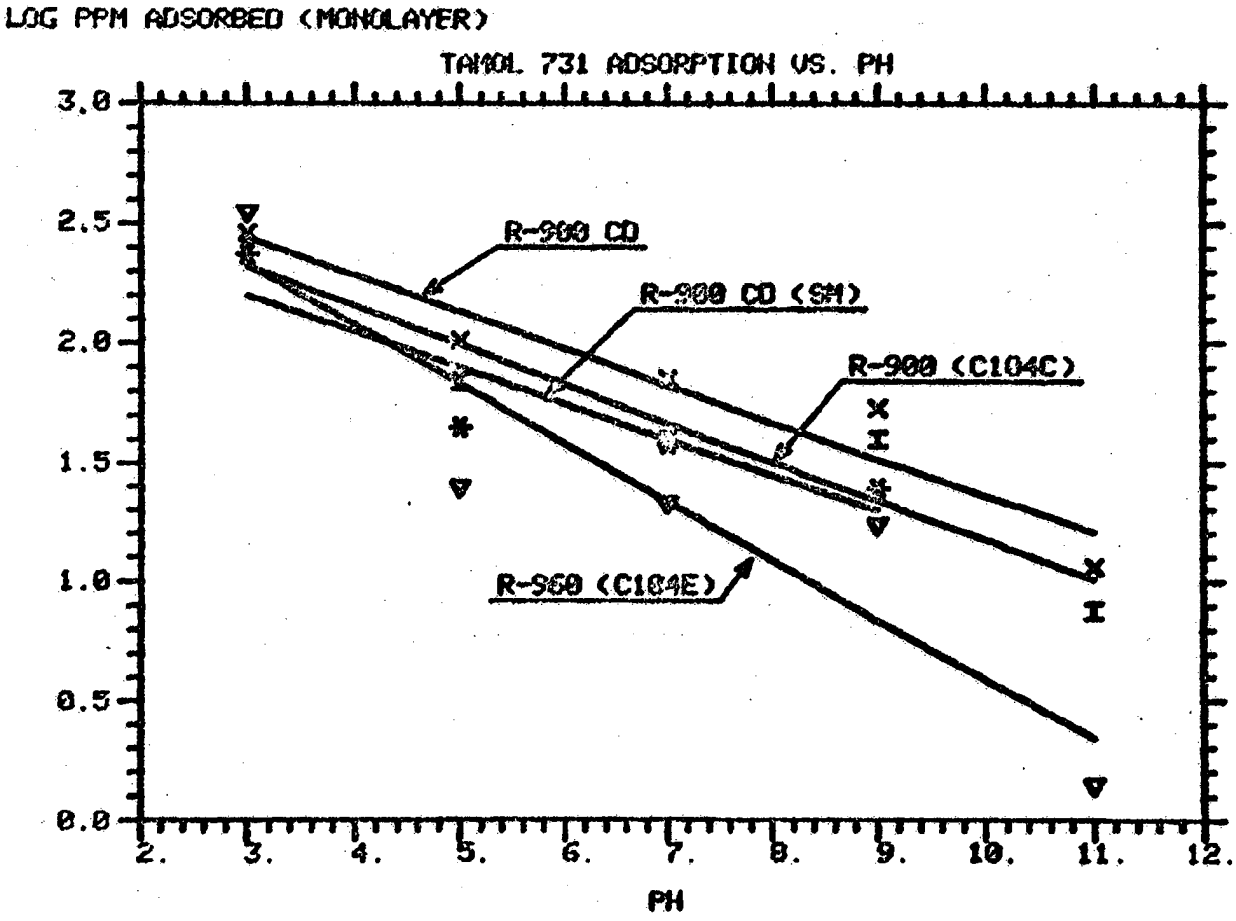
LOG PPM ADSORBED (MONOLAYER)
TAMOL 731 ADSORPTION VS. PH
3.0
2.5
2.0
1.5
1.0
0.5
0.0
2.
3.
4.
5.
6.
7.
8.
9.
10.
11.
12.
PH
R-900 CD
R-900 CD (SM)
R-900 (C104C)
R-960 (C104E)

Figure 29

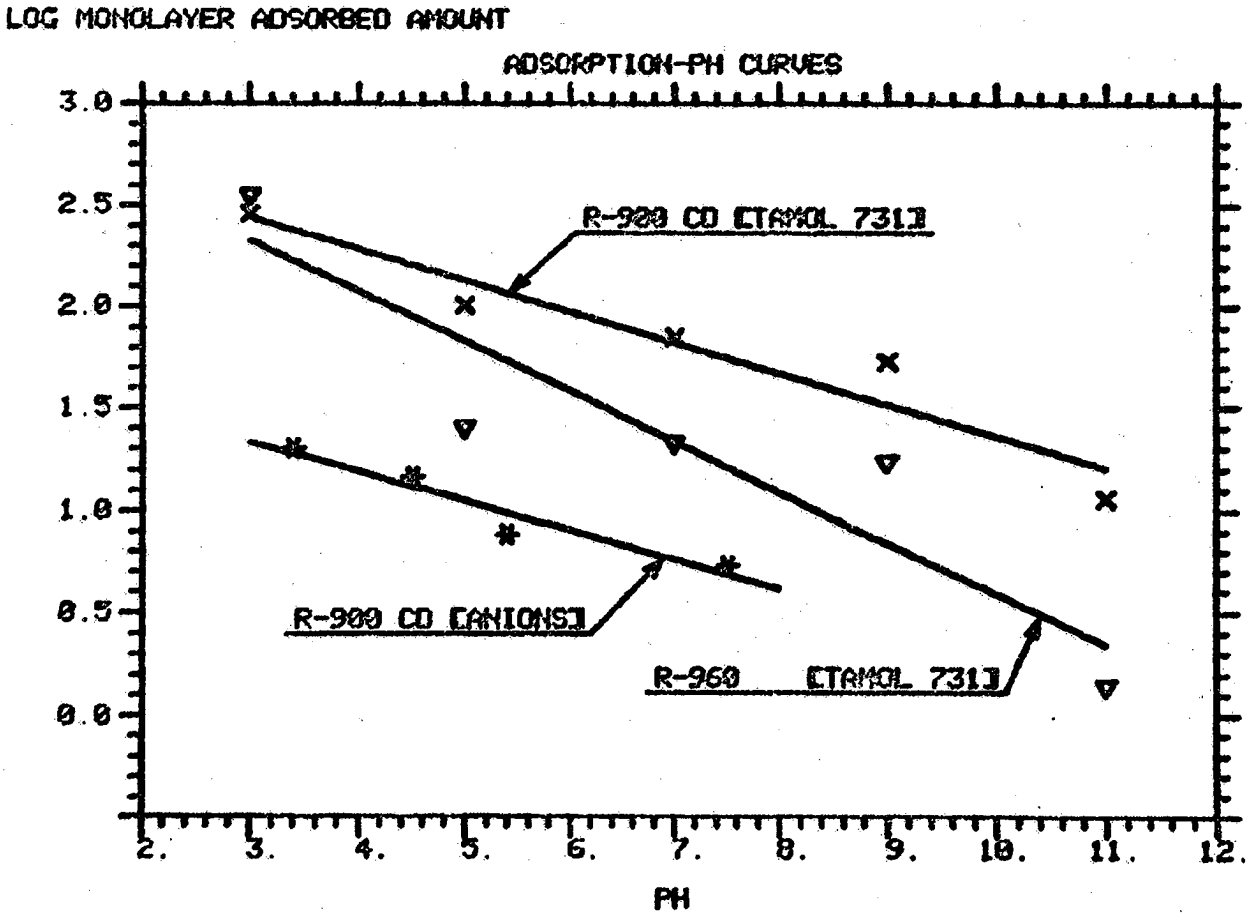
LOG MONOLAYER ADSORBED AMOUNT
ADSORPTION-PH CURVES
3.0
2.5
2.0
1.5
1.0
0.5
0.0
R-900 CD [TAMOL 731]
R-900 CD [ANIONS]
R-960 [TAMOL 731]
2.
3.
4.
5.
6.
7.
8.
9.
10.
11.
12.
PH

Figure 30. R-960 @ pH 3

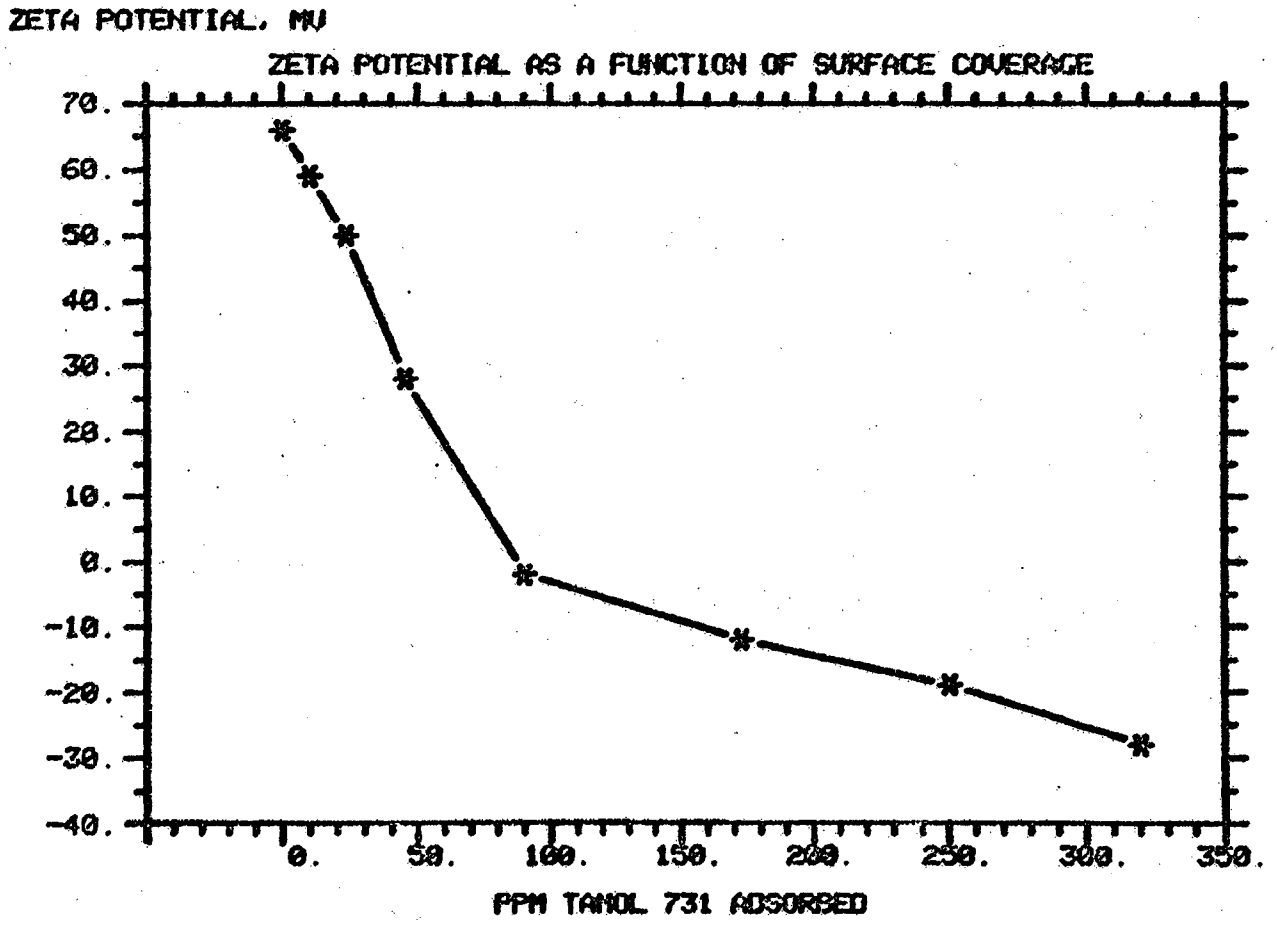

Figure 31. Agglomerate Size Measurement of Suspensions Used to Generate Figure 30

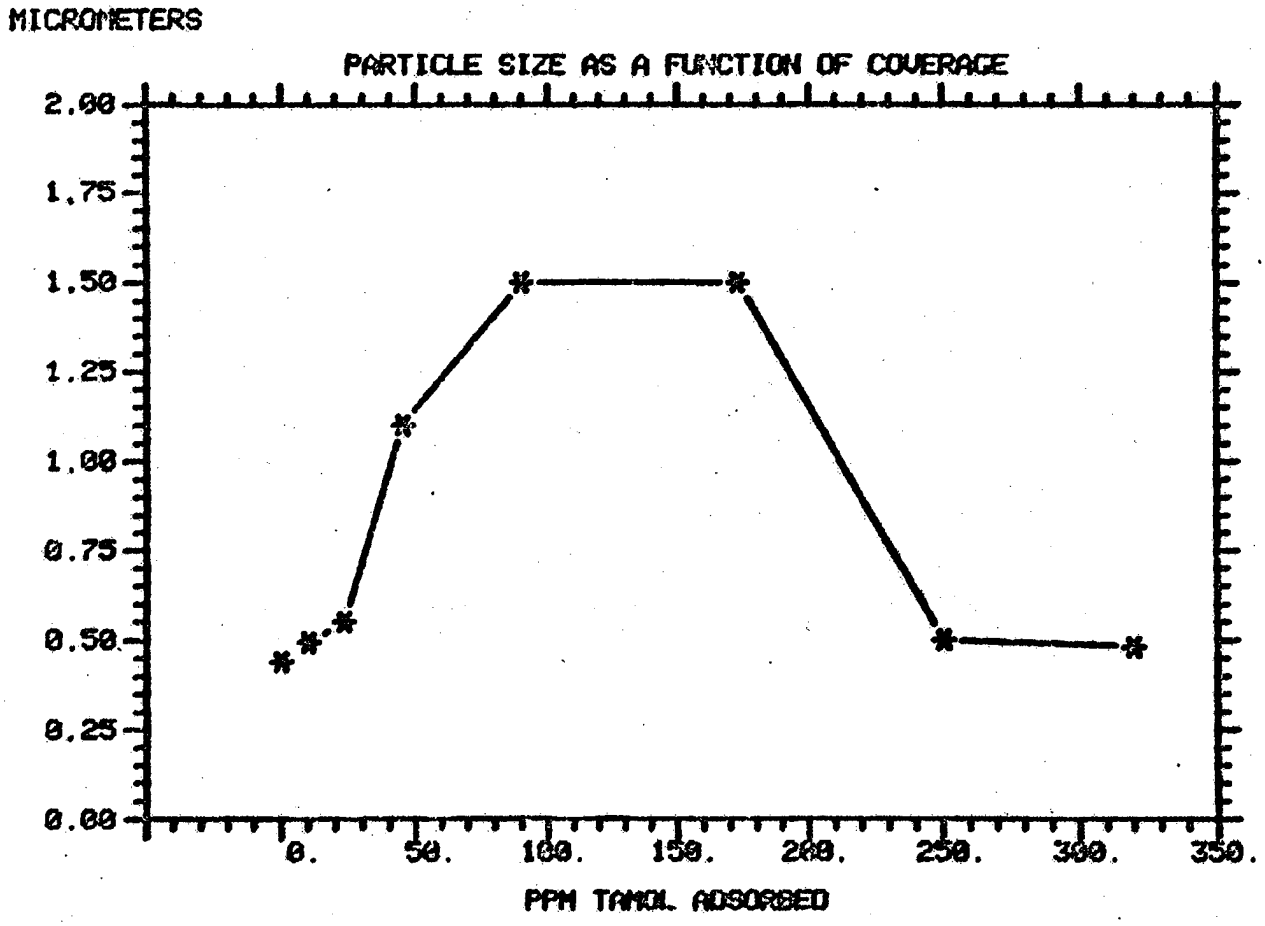

DISTRIBUTION

Copy No.

1. L. Abrams, E356
2. K. K. Bhatia
3. W. J. Marshall, EM
4. H. B. Clark/R. W. Hess
5. R. A. Darby/A. S. Bjornson/L. T. Frick/J. G. Ishikawa
6. E. C. Broge/J. Blackwell/J. A. Blumberg
7. J. M. Hustler
8. L. N. Fisher/G. A. Hapka

9-10. Central Report Index, ISD, C-2311

11-12. L. A. Wierzbowski, EM

13-17. CD&P Information Center, E336

18. R. E. Johnson, CR&DD
19. J. P. Jesson/H. S. Jarrett/R. V. Kasowski/W. F. Jaep, CR&D, E356
20. W. D. Ross/S. V. Mastrangelo/H. R. Linton/D. P. Fields, EM
21. J. H. Boughton
22. W. L. Kremer/G. H. Senkler, EM
23. G. E. Lynskey/D. U. Gwost/M. Baloga, JV
24. D. H. Eastham/T. B. Scarfe/D. P. Schussler, DeL
25. J. G. Dickinson/W. J. McGinnis, CR
26. CR&DD Tech. Records, E301
27. R. J. Bouchard, CR&DD